IJNRD.ORG ISSN : 2456-4184
INTERNATIONAL JOURNAL OF NOVEL RESEARCH AND DEVELOPMENT (IJNRD) | IJNRD.ORG
An International Open Access, Peer-reviewed, Refereed Journal

REMOVAL OF WATER HARDNESS USING A COMPOSITE OF SODIUM SULPHONATED POLYSTYRENE RESIN AND MORINGA OLEIFERA SEEDS POWDER

S.M Mutyanda, D.NYAMA and A.Maringa

Department of Applied Chemistry, National University of Science and Technology, Bulawayo, Zimbabwe

Abstract

Sodium Sulphonated Polystyrene Resin and Moringa Seed Powder were used to soften hard water. Polystyrene sulphonation was investigated across a range of periods, including 1, 2, 3, 4, and 6 hours. At the 4-hour intervals, there was a significant amount of sulphonation (24.5%). At a 4 hour interval, the cation exchange capacity was 1.6 meq/g. At 4 hours, there was a significant degree of edema that was 411%. Through the use of experimental testing, the effects of adsorbent dose, pH, contact duration, metal ion concentrations, and temperature on adsorption effectiveness were investigated. The highest equilibrium absorption of Ca^{2+} and Mg^{2+} by the adsorbent was 92.5% at the optimal pH of 7, contact period of 150 minutes, and temperature of 25^{o}C 0.5 $\pm^{o}$C. Fourier transform infrared (FTIR), thermo gravimetric analysis (TGA), and X-ray powder diffraction were used to establish the composite's structural integrity (XRD). Several isotherm models were used to analyze equilibrium adsorption; the Freundlich isotherm with R2=0. 9712 was found to be the most favorable one. According to the Dubinin-Radushkrvich isotherm, which had an E value of 31.6 kJ/mol, the adsorption was verified to be caused by physisorption. Redlinch Peterson's B=0.4 result also provided support for the multilayer adsorption. Additionally, supporting multilayer adsorption was the Halsey isotherm, with R^2 = 0.9596. R^2=0.9406 revealed that the kinetic model was of the first order. The fact that the graph did not pass through the origin indicates that the intra particle diffusion and other kinetic processes were to blame. The reaction was endothermic because H=8.041KJ/mol, according to studies on thermodynamics.. The fact that H was less than 40 kJ/mol further reinforced the idea that the mechanism was physisorption. The results show an improvement in the level of freedom of adsorbed species. It shows that the proportion of adsorption rises with temperature. The fact that the Gibbs free energy is negative indicates that the adsorption process is thermodynamically possible, and the degree of spontaneous increase with temperature. Titration and Flame Atomic Absorption Spectrometry (FAAS) techniques, respectively, revealed that the total water hardness before adsorption was 1080 mg/l and 1272 mg/l. Using the titration and FAAS methods, it was determined that the concentration after adsorption was 216 mg/l and 400 mg/l, respectively. This might reduce water hardness by 78% to 80%. The amount of total chlorides was determined to be 313.11 mg/l prior to adsorption and 0 mg/l following adsorption, suggesting that all chlorides were eliminated from the water.

Keywords, Sodium, Sulphonated, Polystyrene resin, Ion exchange capacity

1. Introduction

Groundwater has become a crucial resource for residential supplies. 20–40% of the world's drinking water comes from groundwater (Margat, 2013). According to UNICEF (2012), groundwater contributes to around 63.1% of the water consumed in metropolitan areas. Disease outbreaks were mostly brought on by the usage of subsurface water, according to (Gleick, 2003) and (Soren, 2011). Rao (2004) and Foster (2010) claim that a country's inability to offer enough clean water to its citizens as a result of the increasing consumption of subsurface water. Van Der Hoven (2004) and Schot (2012) reviews found that pollution causes temporary quality decline in urban ground water. According to Plonke (1985) and Lerner (2009), the dynamic interaction of several legal and illegal land uses with rainfall, runoff, and the process of ground water recharge results in ground water contamination. All water samples tested from Gweru boreholes,

according to study by (Mukanga, 2016), showed total water hardness levels that were greater than recommended.

Table 1: Ground water total hardness classes in Gweru City

Total water hardness	Class	Borehole location
0-75	Soft	None
75-150	Moderately hard	Mkoba ll, Riverside
150-300	Hard	Mkoba19,20 and Lundi Park
>	Very hard	Senga, Mambo, Mkoba 13 andNashville

The felsite and porphyries, which are naturally occurring rocks rich in magnesium, calcium, sodium, and potassium, are the cause of the hardness of the water. Water hardness is caused by the weathering of the metal ions Mg^{2+} and Ca^{2+} from the rocks. According to UNICEF (2012), 1 in 8 people lack access to clean drinking water, and a sizable portion drink hard water. In 2013, Tamrakar and Shakya provided evidence that Ca^{2+} and Mg^{2+} contamination of ground water in numerous locations of Nepal contributes to the high degree of water hardness. Out of 270 water samples, 60, 20 and 10% of the samples from wells, streams, and springs, respectively, exhibited hardness levels over 180 mg/l (Tamrakar, 2013). In Kathmandu, water samples from wells were analyzed for water hardness, and it was discovered that 50% of the samples had water hardness more than 180 mg/l. The Kathmandu Valley's groundwater has a hardness level of up to 800 mg/l, according to Pant (2011). Hard water affects all household tasks, including laundry, bathing, and dishwashing, by reducing the cleaning power of soap. According to (Suzuki, 2002). It has been found that the heating of hard water causes the formation of lime scale deposits. Due to the obvious precipitates they leave behind, such as salts or insoluble soaps, these deposits can cause problems with the operation of water-using appliances. Suzuki (2002) examined the idea that water hardness also contributes to the buildup of scale in hot water lines, requiring routine pipe replacement. Water pumps' effectiveness and performance may suffer as a result of scale buildup. Precipitation formation may result in a reduction in the boiler's ability to transmit heat, a slowing of fluid flow, water pipeline breaches, and the development of stains on dishes and clothing. A high magnesium content in drinking water may cause a bitter taste (Dimirkou, 2008). The use of Sodium Sulphonated Polystrene resin-Moringa seed Powder (NaSPR-MSP) composite will address the financial problem of importing resin for water treatment. because moringa seeds and unwanted polystyrene products are recycled to become useful materials rather than being discharged into the environment. Moringa seed powder is useless for humans in terms of food and medication. . The only oil utilized for cooking and lighting is that which is extracted from Moringa seeds. The Council for Scientific and Industrial Research claims that the oil may also be used in cosmetics, but that it is useless for softening or treating water. This opens up the possibility of using moringa seed powder for water purification. This study will make use of the waste polystyrene, which is contaminating the environment and causing Zimbabwe problems. There are now restrictions on the use of polystyrene in food applications, and there are limitations on the potential uses of recycled polystyrene, which can only be used for packaging, insulation, floating billets or boards, future, and drainage tiles. The creation of a complex combination of polyaromatic hydrocarbons (PAHS) during the incineration of waste polystyrene, especially at low temperatures, has drawn criticism (800 - 900oC). When breathed, PAHs have been shown to cause genotoxicity and carcinogenicity (Durlak S, 1998).

According to Hocking, the adoption of paper packaging as a substitute for polystyrene in packaging has helped most nations, including the USA, reduce the threats to the public's health posed by PAHs. The usage of Styrofoam, commonly known as polystyrene, is prohibited in several nations, including Zimbabwe, the USA, and India, as part of their certification requirements. Before 2007, Taiwan forbade the use of polystyrene foam in restaurant service (Quan, June 13 2006).

2. Material and Methodology

2.1 Sampling

Waste polystyrene plastics were sampled from residential bins in Cowdray Park, municipal trash sites, and the sides of the road. Sampling was done based on discretion.

2.2 Cleaning of waste Polystyrene material

The plastics were washed with distilled water and detergent after being torn into smaller pierces. With new distilled water and detergent solution, the process was carried again four more times. They were cleaned, washed with distilled water, and then dried in an oven at 60°C for 30 minutes, or until they were completely dry. Clean polythene plastic bags were used to package the cleaned plastics in order to prevent contamination pending further inspection.

2.3 Synthesis of waste polystyrene resin (WPS**)**

A 500 ml beaker containing 15 grams of discarded polystyrene plastics was filled first, and then 300 ml of 98% concentrated sulfuric acid was added. WPS were allowed to react at room temperature for six hours. After that, the slurry was six times rinsed in 250 ml of distilled water and filtered using a filter funnel. To guarantee that resin was removed, the pH paper was used to test the amount of acidity that was still present in washing water. Following a 2- hour reaction with a 1M NaCl solution, the resin underwent a 30-minute drying process at 60°C.

2.4 Preparation of Moringa seed powder

The powder was made by employing the Soxhlet method to extract the oil from the moringa seed. The extraction thimble held 20 grams of powdered seed. 340 cc of the solvent hexane were placed in a flask with a circular bottom. A heater was used to heat the solvent; it was activated when the solvent reached boiling point. The oil was eliminated within 45 minutes. The procedure was carried out four times to obtain a sample of 100 grams of Moringa seed powder, which was then taken out of the thimble, washed with distilled water, and allowed to dry for a whole night at 50°C inthe oven.

2.5 Characterization

FTIR, XRD, and TGA were used to characterize synthetic polystyrene resin, Moringa seed powder, and a mixture of the two. FTIR, XRD, and TGA were also used to analyze the composite before and after adsorption

2.6 Preparation of synthetic hard water

In 1000 ml of distilled water, magnesium chloride (1.0079 g) and calcium chloride (1.0056 g) were dissolved while being agitated with a magnetic stirrer. The solution was then filtered using two layers of filter paper.

2.7 Total hardness determination

Titration of prepared hard water with a 0.00991M EDTA solution was used to calculate total hardness. A volumetric flask that was empty was filled with 25 ml of prepared hard water. Following this, 2ml of ammonium buffer and a few drops of Eriochrome black T were added, causing the solution to become red. Once blue color was seen, indicating the end point, the solution was then titrated with 0.00991M EDTA. The same procedure was used three times, recording the starting and ending volume values on a table of values. The average volume was used to determine thetotal hardness.

2.8 Water hardness removal

A composite resin made of Moring and Polystyrene in various weight ratios was prepared to test the removal of water hardness. Moringa and sodium polystyrene resin of ratio 3: 1 respectively, moringa and sodium polystyrene resin of ratio1: 3 respectively, moringa and sodium polystyrene resin of ratio 1:1, moringa and sodium polystyrene resin were prepared, and each was then added into plastic containers each containing 100ml of hard water with a concentration of 1126 mg/l. It took 150 minutes to shake the solution. Following filtration, the overall hardness of the solution was calculated. The previously manufactured hard water was then utilized to create hard water in various concentrations, including 10 mg/l, 20 mg/l, 50 mg/ml, 100 mg/l, 150 mg/l, and 200 mg/l, each of which was created by diluting the previously made hard water by 1126 mg/l.

2.9 Optimization studies

2.9.1 The effect of Time

The impact of time was assessed by treating 100 ml samples of hard water with a concentration of 150 mg/l with a composite of Moringa and sodium Polystrene resin for a duration of 30, 60, 90, 120, 150, 180, and 210 minutes, respectively, using masses of 5.0056g, 5.0074g, 5.0067g, 5.0098g, 5.0056g, 5.0032g, and 5.0024g. Utilizing a 0.00991M EDTA solution, the solution was filtered and titrated.

2.9.2 The effect of pH

Water hardness of 150 mg/l, room temperature, 90 minutes of contact time, and a constant mass of around 5 g were used to analyze the impact of pH on hardness removal. Hard water sample were treated with composite polystyrene resin and Moringa. pH levels 2, 5, 7, 9, and 12 were used to treat the samples of hard water. A titration procedure was used to determine the solution's ultimate concentration after it had been filtered.

2.9.3 The effect of concentration

A total of 1126 mg/l of hard water was diluted to create hard water concentrations of 10, 20, 50, 100, 150, and 200 mg/l. Around 5 g of composite Moringa and polystyrene were used to treat 100 ml of each concentration in a room- temperature environment with a pH of around 5.

2.9.4 The effect of temperature

The effect of temperature on hardness removal was determined by using pH around 5 water hardness of 150 mg/l and contact time of 90 minutes and a constant mass of around 5 g. The composite polystyrene resin and moringa were added to hard water samples. The hard water samples were treated at temperature of 20ºC, 30ºC, 40ºC, 50ºC and 60ºC. The solution were then filtered and final concentration was determined using titration method.

2.9.5 Adsorption equilibrium models

In order to achieve equilibrium, 5 g of Moringa and modified polystyrene were added to a 250 ml conical flask that contained 100 ml of hard water with a concentration of 150 mg/l. To ensure that the greatest amount of sorption was attained, the mixture was shaken at 200 rpm for 120 minutes at 25ºC.When describing the adsorption equilibrium, Langmuir, Freundlich, and Temkin isotherms were used to identify the mechanism for the simultaneous elimination of hardness.

2.9.6 Kinetics modeling

It was possible to study the kinetic adsorption of hard water ions on a composite of Moringa and Modified polystyrene adsorbents by adding 5 g of adsorbent into a 250 ml conical flask containing 150 mg/l of hard water, adjusting the pH to 7, and shaking at 200 rpm for intervals of 30, 60, 90, 120, 150, 180, and 210 minutes. The adsorption kinetics were examined using models of pseudo-first and pseudo-second order.

2.9.7 Thermodynamic parameters for adsorption

The graph of Arrhenius was plotted using $\frac{1}{T}$ against ln (kl). The values of ΔH and ΔS were determined from the slope and intercept of the linear plot of $\frac{1}{T}$ against ln (kl).Calculation of ln (kl) was done using the equation $\ln(kl) = \frac{qe}{ce}$ in which ln(Kl) is related to Arrhenius plot which is shown by the equation $\ln(Kd) = \frac{\Delta S}{R} - \frac{\Delta H}{RT}$.The slope was determined using the equation: Slope$= -\frac{\Delta H}{R}$ and intercept $= \frac{\Delta S}{R}$.In all equations. R is the universal gas constant (8.314 J/K/mol)

2.10 Application of Composite in removal of water hardness removal from borehole

A sample of 100 ml of hard water was mixed with the composite, which has a mass of 5.0025 g. The pH of the solution was 7 after 150 minutes of shaking the sample at room temperature. The solution was then filtered, and the filtrate was diluted to a level of 100 ml in a volumetric flask before being titrated with EDTA

2.10.1 Preparation of Standard for FAAS analysis

2.10.2 Calcium determination

A volumetric flask was used to dissolve 0.0009375 g of $CaCl_2.2H_2O$ into 100 ml of distilled water to create the standard solution, which has a 20 ppm concentration for calcium measurement. Using $C_1V_1=C_2V_2$, the standard solution of 0, 4, 8, and 20 ppm was created from stock solution.

A volumetric flask was used to dissolve 0.0009806 g of $MgCl_2.6H2O$ into 100 ml of distilled water to create the standard solution, which has a concentration of 20 ppm for measuring Mg. Using $C_1V_1=C_2V_2$, the standard solution of 0, 2, 4, 6, 8 and 10 ppm was created from stock solution. Using FAAS, the produced standard solution was evaluated, and a calibration curve was made using concentration and absorbance. The absorbance of a borehole sampleof unknown water and a sample of artificial water were then calculated.

2.10.2 Chloride determination

In order to make silver nitrate solution, 0.425 g was dissolved in a volumetric flask with a 1000 ml capacity. By adding 25 ml of borehole water and a few drops of potassium dichromate to a conical flask, chlorides were then measured. Silver nitrate solution was used to titrate the solution until a brick-red precipitate was produced. The following equation was used to determine the chloride concentration:

$$\frac{Cl}{l}\left(\frac{Mg}{VW}\right) = \frac{(VAg \times NAg \times AR\ Cl) \times 100}{} \qquad (3.10)$$

VAg= volume of silver nitrate usedNAg=Normality of $AgNO_3$ VW=volume of water sample used

3. Results and Discussion

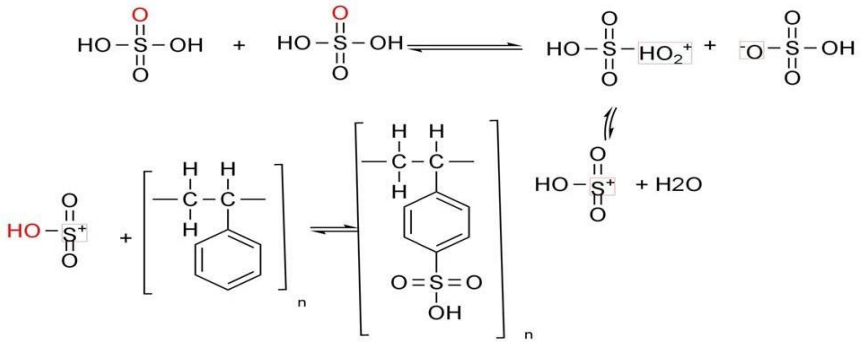

Figure 1: Sulphonation

3.2 Sulphonation of polystyrene**.**

Sulphonation reaction is categorized as aromatic electrophilic substitution reaction. The aim being to substitute H atoms with SO_3H group by chemical bonds on the carbon atoms as shown above. The presence of the sulphonic group causes the polystyrene to have a charged group that can deliver proton. The sulphonation reaction in the polystyrene can occur in ortho and para position to the alky chain. However the substitution reaction is easier to occur in the para due to steric hindrance of the ortho position (Mulijani.S, 2014). The sulphonation reaction at the para position can beseen in the figure 1 above.

3.3 Characterization of Adsorbent using FTIR

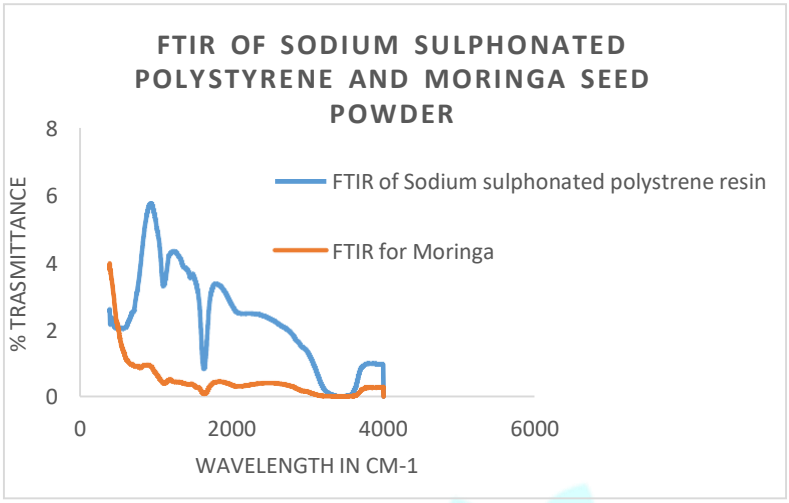

Figure 2: FTIR for Sodium sulphonated polystyrene Resin and Moringa seed powder

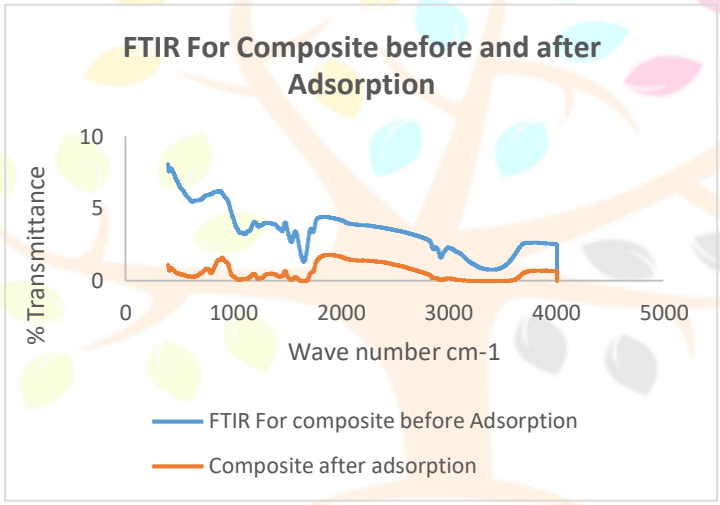

Figure 3: FTIR for Composite of Sodium sulphonated Polystyrene Resin and Moringa Seed Powder before and after adsorption.

The FTIR for sodium sulphonated polystyrene resin showed peaks at 3427.42 cm^{-1} for OH, 1639,78 cm^{-1} for C=C stretching of aromatic ring. The peak at 1108,95 cm^{-1} was for O=S=O in the benzene ring. The FTIR for Moringa seeds powder showed peaks at 3474.90 for OH or N-H group and 1641,97 for C=O group. The composite of NaSPR- MSP before and after adsorption showed new peaks at around 1543.89, 1449.64, 1236.22, 1060.58, 1110.44, 799.74 and 625.86. According to (Bozkurt.A, 2005) The FTIR peaks of composites of NaSP and MSP before and after adsorption shows bands at 3349.00 and 3404.31 respectively this band indicate OH or NH functional group. The absorbing band of in the range 2854-2962 cm^{-1} exhibits vibrational bonds of aliphatic ring. The peak at 1673.40 and 1656.53 indicate C=O group or C=C bonds in aromatic ring. The band located at 1543.49 cm^{-1} is due to the benzene ring stretching. The peaks ranging between 1000 and 1300 cm^{-1} correspond to C-O (ketone). The peaks close to 1060.58 cm^{-1} close to 1058.92 represent C-O cellulose and that at 1236.221 may correspond to C-O-C (cellulose and hemicellulose. The spectra of composite exhibited the characteristic bands at 625.85-799.74 represents the mono substituted aromatic ring of composite (Bozkurt.A, 2005).The decrease in sharpness of the peak at 1640 and decrease

of the broad peak at 3000 showed that the composite had adsorbed calcium and Magnesium ions .The decrease in the transmittance of the composite after adsorption showed that Calcium and Magnesium ion cannot be detected by FTIR.

3.4 Characterization of Adsorbent using TGA

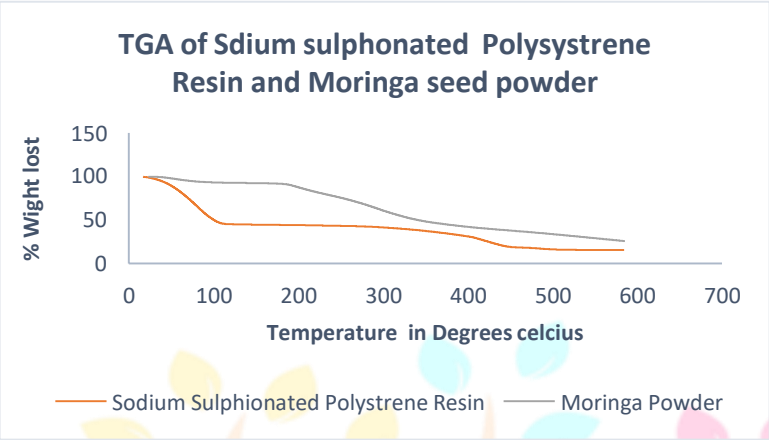

Figure 4: TGA for sodium sulphonated polystyrene and for Moringa seed powder

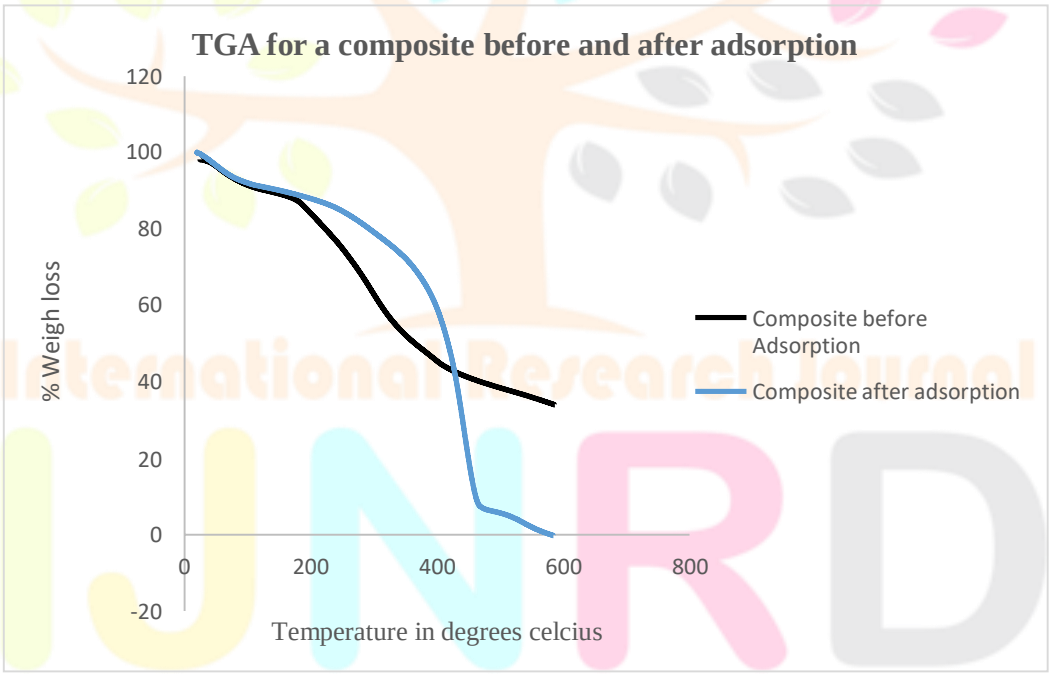

Figure 5: TGA for composite of Sodium Sulphonated Polystyrene Resin and Moringa Seed Powder before and after adsorption

Thermo gravimetric analysis was used to characterize the decomposition stages and thermal stability of Moringa seeds powder, sodium sulphonated polystyrene resin, and composite before and after adsorbent. As shown in Figure 4 the first weight loss for sodium Sulphonated Polystyrene resin from temperature of 0ºC to 100° C with 55% loss was due

to evaporation of water. The second stage from temperature of 100 ºC to 450 ºC with 45 % was due to styrene degradation. The last stage for decomposition was due degradation of sulphonic group from 450 ºC to 575ºC with 5
% loss. The mass loss curve of Moringa seeds powder in figure 4 shows three stages. The first stage from 0 ºC to 100ºC with 10% weight loss was due to evaporation of water according to (Anwa, 2007). The second step from 100 ºC to 325ºC with 55 % weight loss occurs due to the decomposition of organic matter mainly protein components, present in the Moringa seeds and the third stage which occur from 325ºC to 575ºC may be due to decomposition of fatty acids for example oleic acid which has boiling points of 360ºc and gave weight loss of 20%.

In figure 5 the composite sure three sages for weight decomposition. The first decomposition occurs from 4 0ºC to 100 ºC with 20% weight these was due to water evaporation. The second decomposition occurs from temperature of 100ºC to 310ºC this may be due to decomposition of organic compounds and polystyrene and the last decomposition was due to sulphonic acid group and fatty acid group which occurred from 310ºC to 575ºc with 15% loss. The composite after adsorption shows a long temperature range of decomposition from 20ºC to 400ºC with 40% loss this may due decomposition of Ca ions, Mg ions, and protein group. The third temperature range from 400ºC to 450ºC which has contribution of 45% may be due to decomposition of fatty acid group and the decomposition was due decomposition of sulphonic group which occurred at a temperature range of 450ºC to 575ºC.

3.5 Characterisation of Adsorbent using XRD

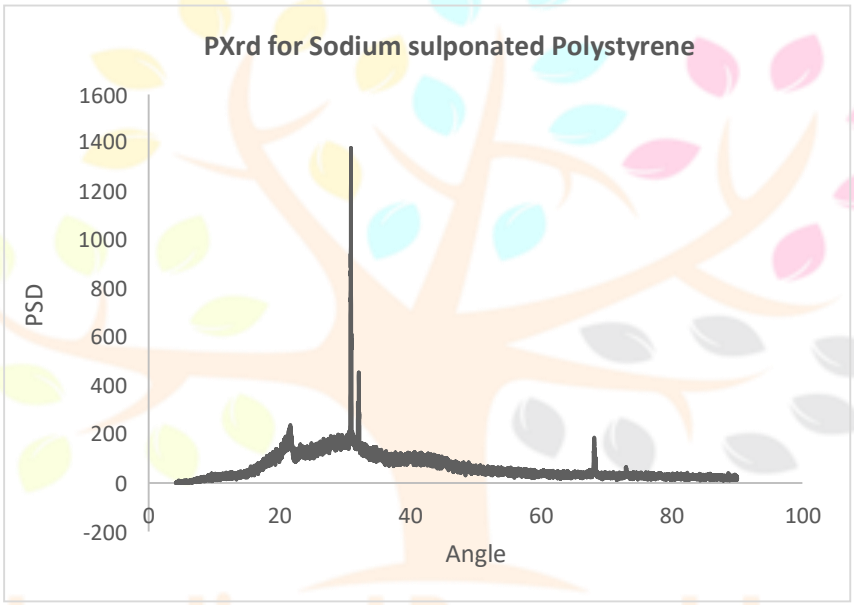

Figure 6: Xrd of Sodium sulphonated Polystyrene

.

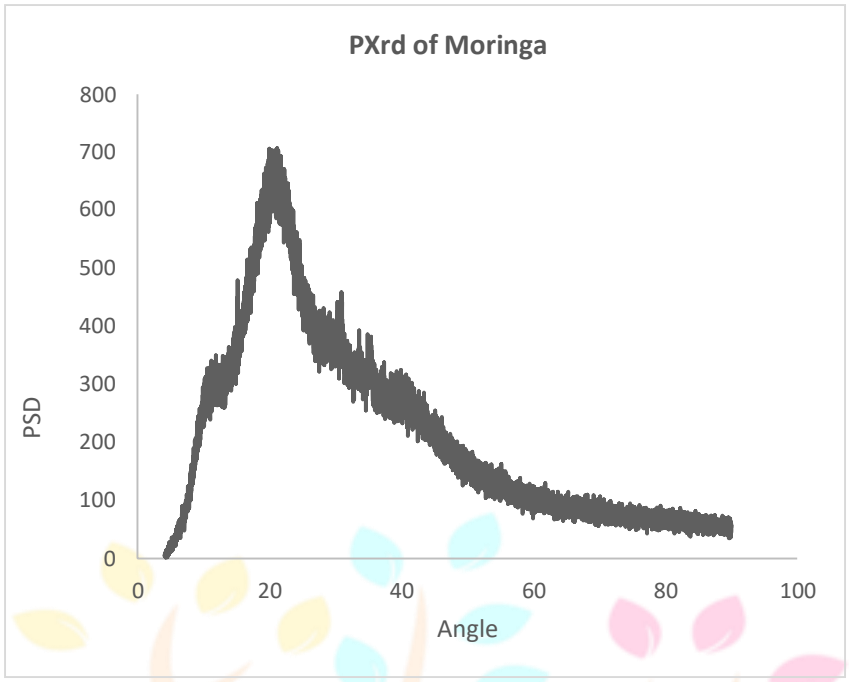

Figure 7: Xrd for Moringa seed Powder

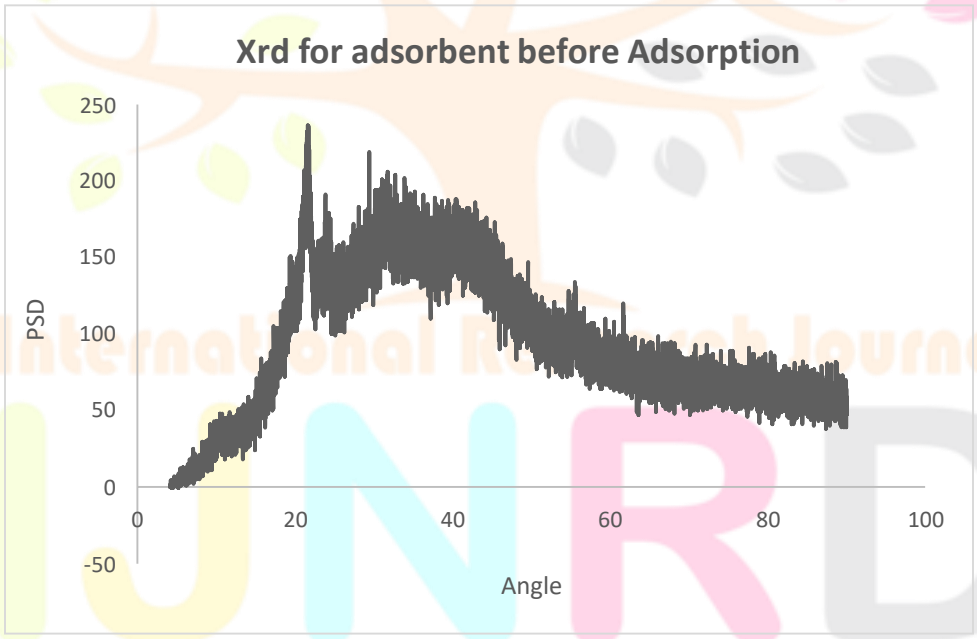

Figure 8: Xrd for composite before adsorption

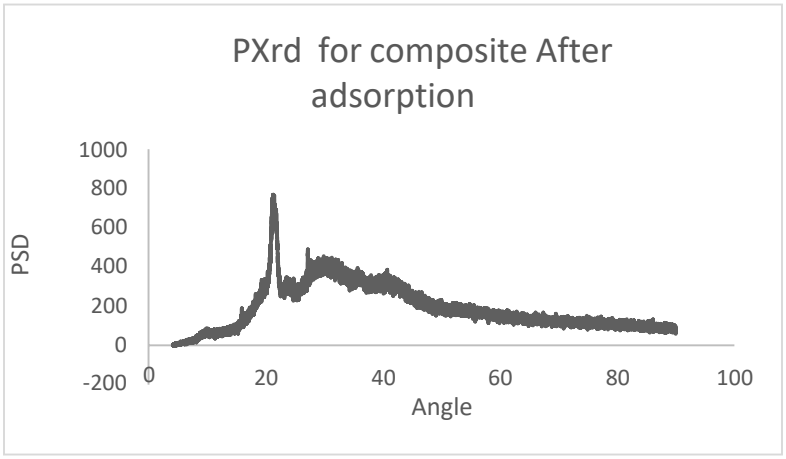

Figure 9: XRD for composite after adsorption.

The XRD was used to determine the morphology of sodium sulphonated polystyrene resin, Moringa seeds powder, adsorbent of sodium sulphonated polystyrene resin and Moringa seed powder before and after adsorption. The XRD diffractrogram of NaSPS in figure 6 shows peaks at 2θ angle =22, 31, 33 and 68°. The shape peaks were due to Sodium chloride used modify sulphonated polystyrene resin. This reduces the amorphous of sulphonated polystyrene resin and shows some crystallinity of NaSPS. In figure 7 the diffractogram of Moringa seed powder showed a broad peak at 2θ=20° and the diffractogram shows that Moringa seed powder has amorphous structure. The Xrd diffractogram of composite adsorbent before adsorption showed narrow sharp peak at 2θ =21° and broad peak at 2θ = 35°. The structure showed that the composite has amorphous structure. After adsorption the composite showed a sharp peak at 2θ =21° and broad peak at 2θ=30°. However the peak was sharper than that before adsorption and the broadness of the peak had reduced compared to that before adsorption.

3.6 Comparing % water hardness removal using different Adsorbent

Where MP=composite of sulphonated polystyrene resin and moringa seed powder, M=Moringa seed powder and P=sodium sulphonated polystyrene

resin

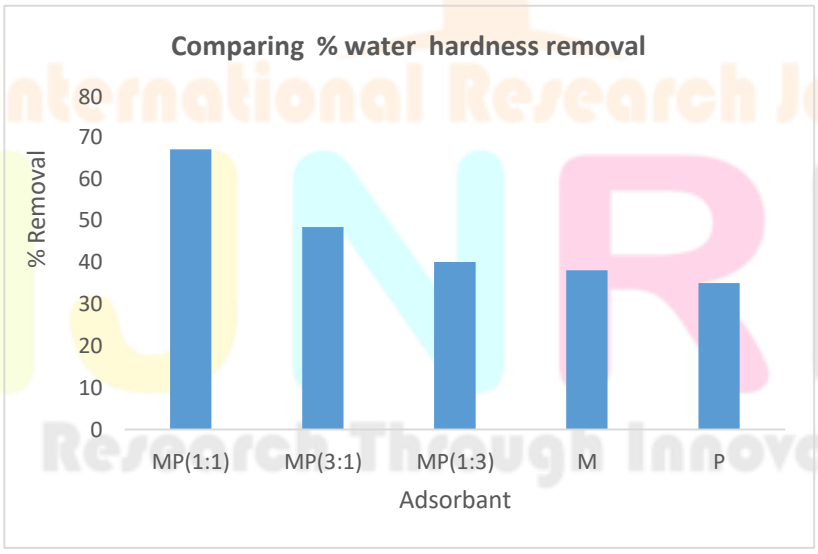

Figure 9: Comparing % water hardness removal of adsorbent

Hard water of 1126 ppm was first synthesized and different adsorbent were then used to determine their potential for removal of hard water. The % removal were found to be 57% for MP (1:1), 46.4 % for MP (3:1) , 38% for MP (1:3) 38 % for M and 35 for P..

Figure 10: Sulphonation of waste Polystyrene resin

Mechanism for synthesis of composite and water hardness removal

The Sulphonated polystyrene resin has crossed linked polystyrene with divinyl benzene and contains sulfonic type functional groups.

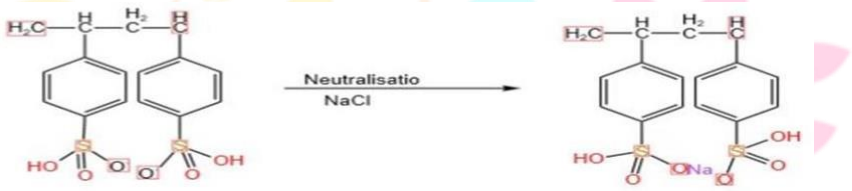

Figure 11: Neutralisation of Sulphonates Polystyrene Resin

The sulphonated polystyrene resin was the neutralized by NaCl to produce NaSWPS which was then used for ion exchange with water hardness cations.

Figure 12: Water hardness removal using Sulphonated Polystyrene.

The water hardness ions from the sample were removed with resin occurred through mechanism that do not involve new chemical reactions but only ion excharge reactions with participation of the functional groups which results in a rearrangement of surrounding water molecules as a result of ion exchange process. According to Dean and Bekri- Abbes et al the FTIR peaks associated with chemical bonding in this type of material are well known and the same observations were made by (Lilian, 2014).

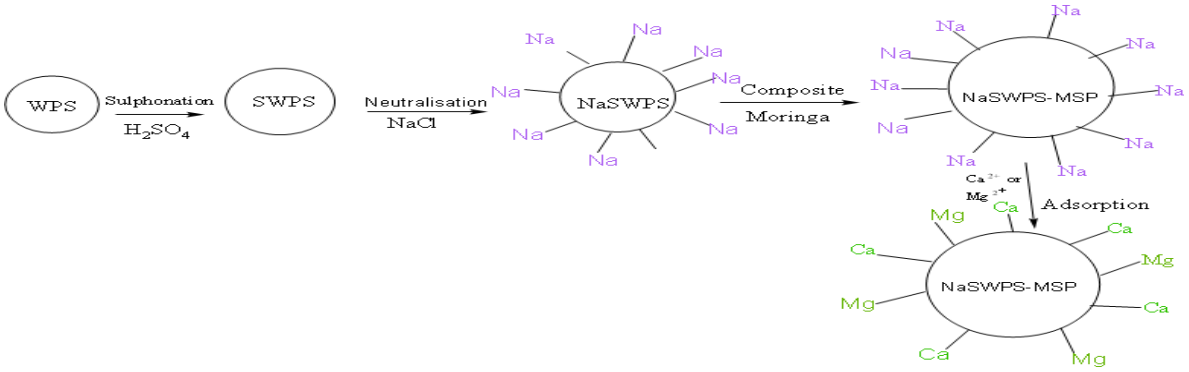

Figure 12: Schematic diagram for composite of sodium sulphonated polystyrene resin and Moringa Seeds Powder for Ca^{2+} and Mg^{2+} removal

The schematic diagram shows that the surface area of combine Moringa and SWPS resin is higher than that of WPS. The sodium ions on the surface could be substituted easily by calcium or magnesium ions. The combined resin of NaSWPS and MSP has smaller random pores indicating that the composite has a large surface area to increase the contact between ions and improving the efficiency of water hardness removal.

3.7 Adsorption Parameters of Sodium Sulphonated Polystyrene Resin and Moringa Seed Powder (NaSPR-MSP).3.7.1.Effects of Dosage

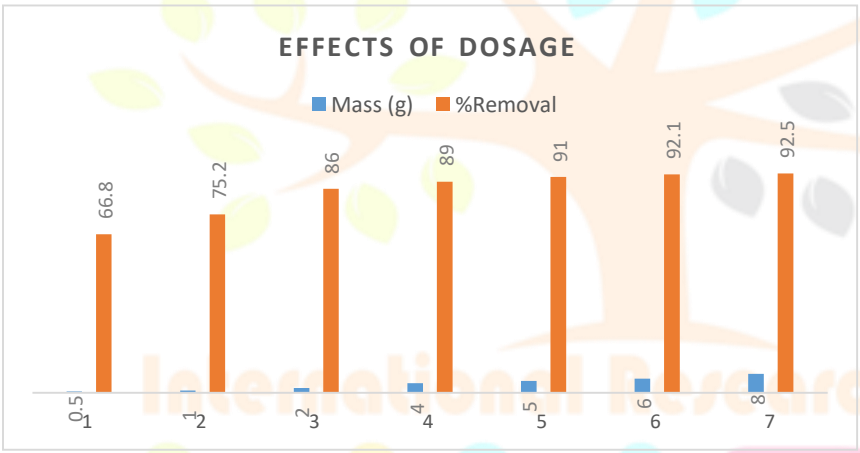

Figure 13: effects of dosage on composite NaSPR-MSP for water hardness removal

The amount of dose utilized was shown to increase the percentage of water hardness reduction. The amount adsorbed ranged from 0.5 to 8 g. using a dose of mass 8 +/- 0.1 g, the greatest removal percentage of 92.5% was noted. The percentage removal marginally increased after the mass of 5 g, demonstrating that further adsorbent increase generates minimal further adsorption. Ca^{2+} and Mg^{2+} have access to more adsorption sites when the adsorbent dose is greater. According to Sarma and Chakrabarty the maximum quantity of adsorption is reached at a given dose of adsorbent, therefore the number of ions stays constant even after adding more adsorbent. This explains why a 5 g mass generated a very slight increase in elimination. An explanation for the observation is by overlapping of adsorption sites as a results of overcrowding of adsorption particles.

3.7.2 Effects of time on water hardness removal

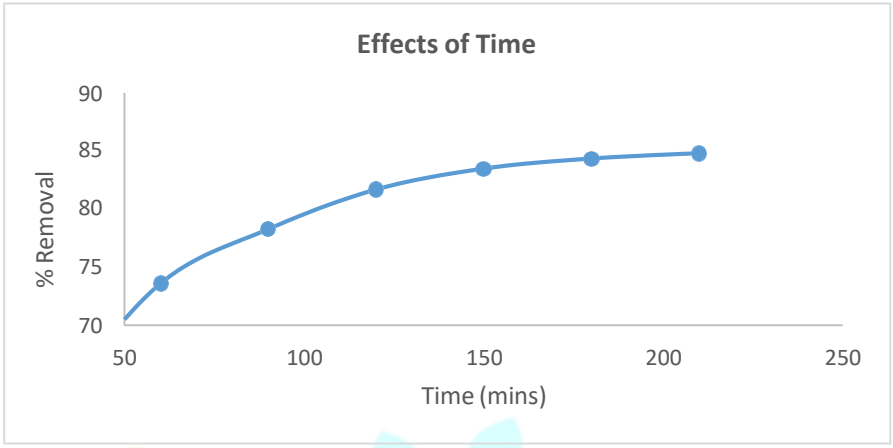

Figure 14: Effect of time on water hardness removal using NaSPR-MSP

At intervals of 30 minutes, the impact of time was examined at a temperature of around 25 ºC, with an initial concentration of 150 mg/l and a pH of 7 0.5. By altering the time from 30 minutes to 210 minutes while holding the other parameters constant, the impact of interaction time was explored. The correlation between contact time and the effectiveness of hardness reduction is shown in Fig. 30. The finding shows that as contact duration grew, hardness ions were removed more effectively. The percentage removal was 88% at the period of 210 minutes, which was the greatest percentage removal. Since there is a little rise after 150 minutes, the optimal period in this study was determined to be 150 minutes. Within 150 minutes, the percentage hardness elimination had reached equilibrium. Further extending the contact duration did not reveal any appreciable changes in the hardness of the water. The difference in the amount of adsorption may be caused by the fact that at first, the solute concentration gradient was strong and all sites on the adsorbent surface were unoccupied. It was discovered that the optimal condition is when the period of reaction is 150 minutes, where by extending the time of reaction, reactants push to the right and the product yield rise. According to Liu et al. (2013), as the time grows, the capacity of water hardness removal also increases. The greatest removal efficiency of Ca^{2+} and Mg^{2+} ions is shown in one of the experiments by Farmanbordar et al. (2016). Occurred in a pH range of 11, between 50 and 95%, and under optimal circumstances. The reaction time was 15 minutes. According to Pujiastuti et al. (2016), a pH range above 9 and a removal capacity of 97% were used to determine the influence of reaction duration on the percentage removal rate of Mg^{2+}. This shows that Mg2+ forms homogenously under specific circumstances and that nucleation occurs quickly. Additionally, it was noted that occasionally the reaction time exceeded 30 minutes because, as stated by Wang et al. (2013), the elimination of Ca2+ ions requires a certain amount of time.30 minutes from waste. There are several studies by Ashley et al 2009, Kurosaki 2003 and Jenkins 1998 in the past mentioned the varying reaction and in this study's optimum conditions was at timeof 120 minutes

The reaction of the exchange is as shown in equation:

$$2ReNa + CaCl_2 \longrightarrow 2ReCa + 2NaCl \quad (4.3)$$

3.7.3 Effects of Temperature on water hardness removal using composite of Sodium Sulphonated Polystyrene Resinand Moringa Seed Powder**.**

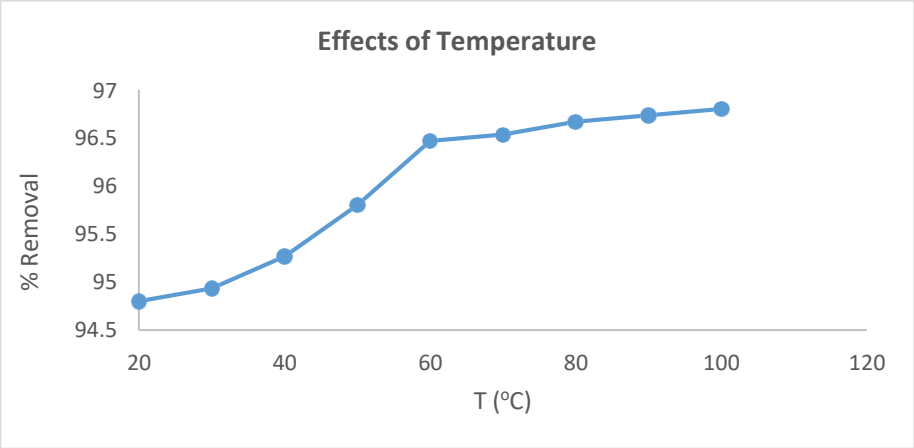

Figure 15: Effects of temperature on water hardness removal using composite of Sodium Sulphonated polystyrene Resin and Moringa Seed Powder**.**

The effects of temperature on the hardness ions' ability to adhere to Moringa and modified polystyrene resin were investigated by conducting experiments at various temperatures of 20 ºC, 30, 40 ºC, 50 ºC, 60 ºC, 70 ºC, 80 ºC, 90 ºC, and 100 ºC, as shown in Fig. 4.20. It was found that when temperature rose, the percentage of hardness removed increased. It was shown that adsorption of hardness ions increased somewhat as temperature rises.

This finding may be caused by the adsorbent swelling, which would then make more active sites available for the adsorption of hardness ions (Sivakumar.V, 2014). Additionally, the latter discovery demonstrates that the endothermic nature of the hardness ion adsorption by Moringa and modified sulphonated polystyrene resin. This is because water hardness adsorption rises with temperature, as shown by (Mohammad et al 2013). The increase in removal efficiency with increase in temperature shows that the Ca^{2+} and Mg^{2+} is endothermic in nature.

3.7.4 Effects of pH on water hardness removal using NaPSR-MSP

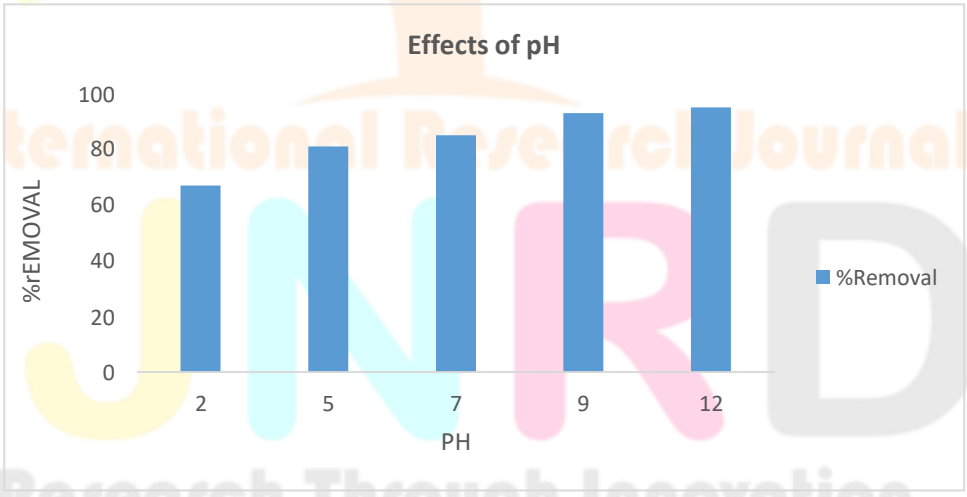

Figure 16: Effects of pH on water hardness removal using composite of Sodium Sulphonated polystyrene Resin and Moringa seeds Powder**.**

With increasing pH, more water hardness is removed on a percentage basis. 95 percent was the highest percentage for removing water hardness at a pH of 11, according to Figure 4.21, which illustrated the impacts of various pH levels.

The number of metal ion binding sites on the adsorbent surface is impacted by variations in hydrogen ions. By adding hydrochloric acid or sodium hydroxide solutions, the initial pH of the hard water solution was managed with a pH meter. In this experiment, the temperature, reaction duration, and resin dose were held constant. The hard water volume was 100 ml, and the adsorbent mass was 5 g. Figure 16 depicts the results of varying pH levels from (2 to 12). The pH of a solution is a crucial factor in the adsorption, as stated by (Maicaneanu.A, 2014). According to the study's findings, the pH of the solution had a significant impact on the elimination of water hardness ions. The reason for this is because changes in hydrogen ion concentration have an impact on the quantity of metal ion binding sites on the adsorbent surface. At lower pH levels, hydrogen ions (H+) surround the adsorbent's surface. According to, the latter inhibits hardness ions from adhering to the binding sites of the adsorbent by repulsion, and, the concentration of H+ decreases with increasing pH (Maicaneanu.A, 2014).

The decrease in competition between positively charged Ca^{2+} and Mg^{2+} ions and hydroxonium ions H_3O^+ at the surface of modified sulphonated polystyrene resin and Moringa leaves may account for the improvement in hardness removal (22). Because of this, it is likely that hardness ions (Ca^{2+} and Mg^{2+}) will become significantly more adsorbent as pH rises. It is possible that the almost equal concentration of H_3O^+ and OH^- ions in the bulk solution, which affects the polarity of the adsorbent and makes it almost too neutral to adsorb additional ions, is the reason why the pH is practically constant between pH 5 and pH 9. The reason why the pH is practically constant between pH 5 and pH 9 may be due to the nearly equal concentration of H_3O+ and OH- ions in the bulk solution, which affects the polarity of the adsorbent and makes it almost too neutral to adsorb additional ions. It is possible that the increased hydroxyl ion (OH-) concentration in the solution, which raises the negativity of the adsorbents, is what caused the rise in ion adsorption from pH 9 to 12.The pH of 12 produced the maximum water hardness reduction of 95%. Due to the necessity to elevate the pH of the water before softening and lower it to neutral pH after softening, this pH does not appear to be both inexpensive and safe. Chemicals used to modify the pH of the water have an adverse effect and lessen the water's safety. Furthermore, additional costs must be invested to purchase the chemicals needed for pH correction. So it's crucial to think about softening at a neutral pH to provide safe water in an affordable and secure manner. Using the data, it was determined that the percentage removal at neutral pH was 85% greater than the 65% Rolence recorded in 2014 using coconut shell.

3.7.5 Effects of Concentration on water hardness removal using NaSPR-MSP

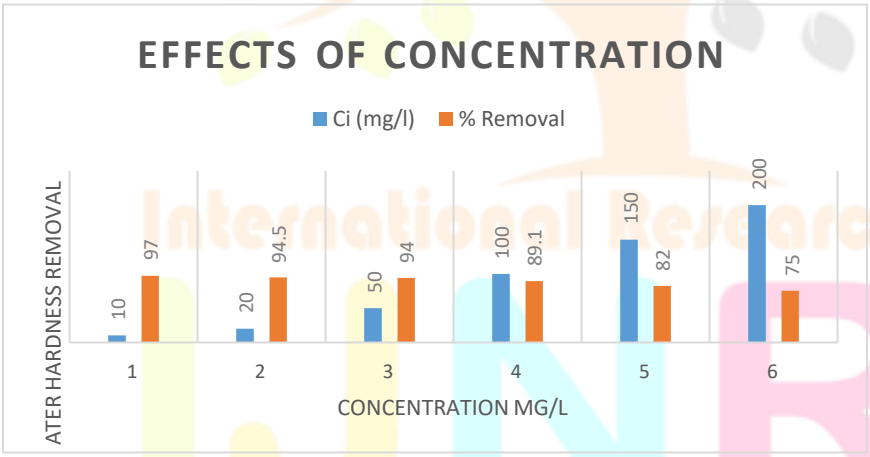

Figure 17: effects of concentration on water removal using composite of Sodium Sulphonated polystyrene Resin and Moringa seeds Powder.

Water hardness that ranges from 10 to 200 mg/l at room temperature, with an optimum 150-minute time, an ideal pH of 7, and a composite mass of 5g. According to the graph above, the percentage of removal decreased from 97% to 75% as the initial concentration of water hardness increased from 10 to 200 mg/l. In solution water hardness ions

would surround the built adsorbent's active site more often and at higher initial concentrations. The NaSPR-MPS composite's equilibrium adsorption capacity grows with increasing water hardness ion concentrations, hastening the adsorption process (Ghorbani.F, 2008). Water hardness percentage decreases as beginning metal concentration increases. When the initial concentration is low, the ratio of the initial number of water hardness ions to the active sites that are accessible therefore the higher removal efficiency of water hardness ions is higher and at higher concentration, further residual of water hardness ions remain in the aqueous solution (Radnia.H, 2012)

3.8 Adsorption Isotherms

Table 2: Parameter for linear adsorption isotherms

Isotherm	Parameter	Value
Langmuir	Intercept	0.01107
	Slope	0.02885
	qmax(mg/l)	34.66205
	KL	1
	RL	0.019608
	R^2	0.9461
Freundlinch	Intercept	1.1354
	Slope	0.55426
	1/n	0.55426
	Kf	20.67283
	R^2	0.9712
Redlich-Peterson (R-P)	Intercept	-3.0288
	Slope	0.44574
	B	0.44574
	A	20.67241
	R^2	0.9562
Halsey	Intercept	28.00218
	Slope	28.73944
	K	0.35832
	R^2	0.9596
Dubinin –R	Intercept	6.4688

	Slope	-0.005
	E	31.62278
	R^2	0.81308
Temkin	Intercept	28.00218
	Slope	28.73944
	BT(J/mol)	28.73944
	KT (mg/l)	2.649436
	R^2	0.94948

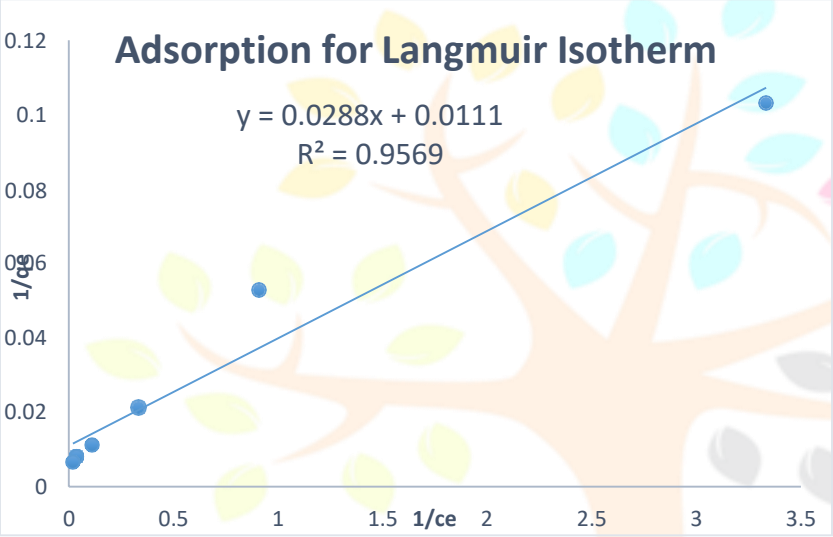

Figure 18: linear isotherm of Langmuir on water hardness removal using NaSPR-MPS.

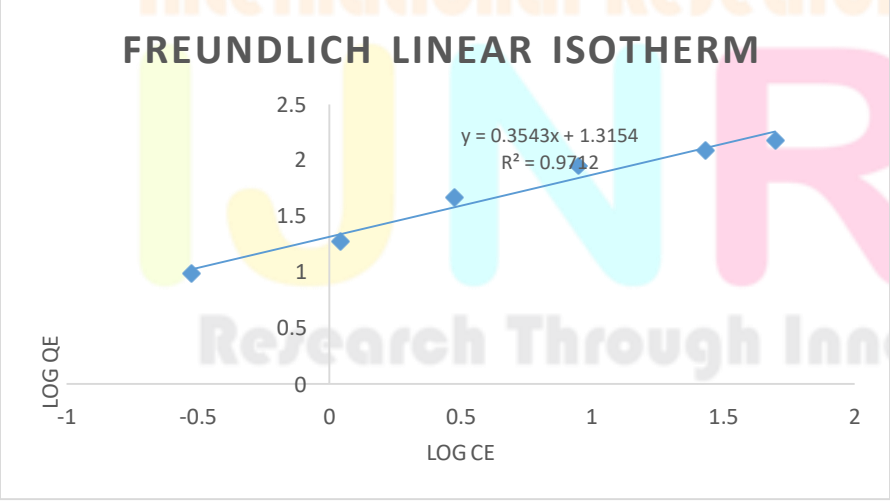

Figure 19: Freundlich linear isotherm on water hardness removal using NaSPR-MPS.

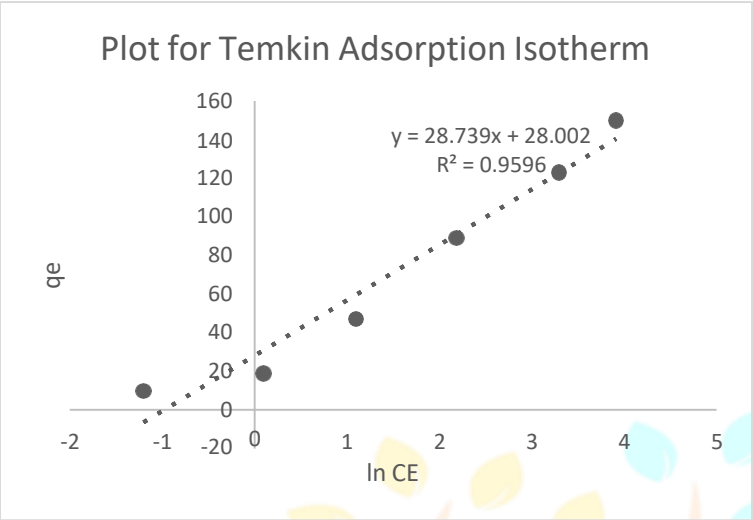

Figure 20: Temkin Linear isotherm on water hardness removal using NaSPR-MPS.

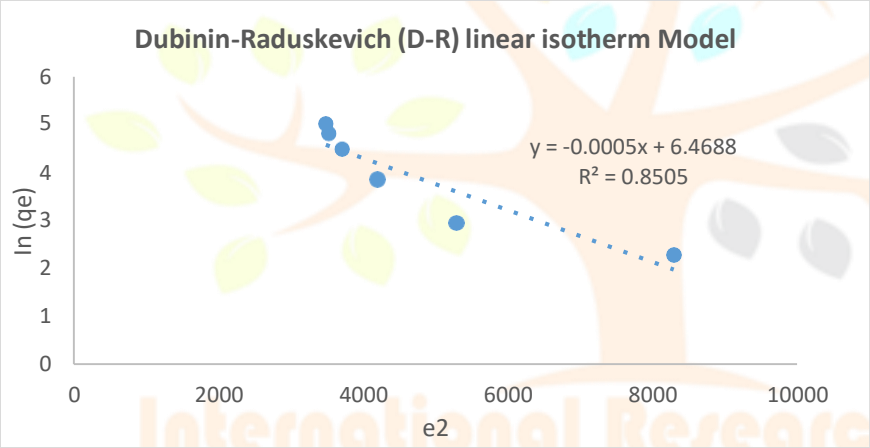

Figure 21: Dubinin-Raduskevich (D-R) linear isotherm on water hardness removal using NaSPR-MPS.

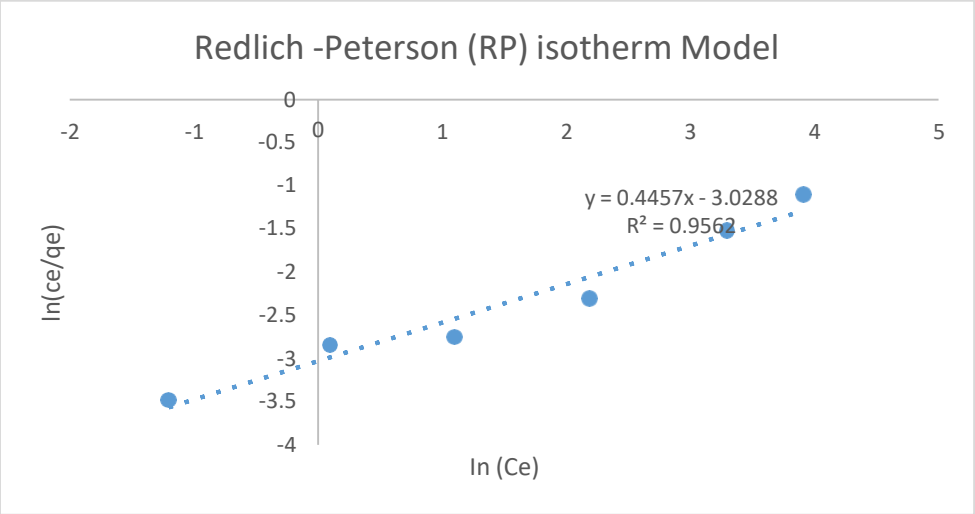

Figure 22: Redlich-Peterson (RP) linear Isotherm on water hardness removal using NaSPR-MPS.

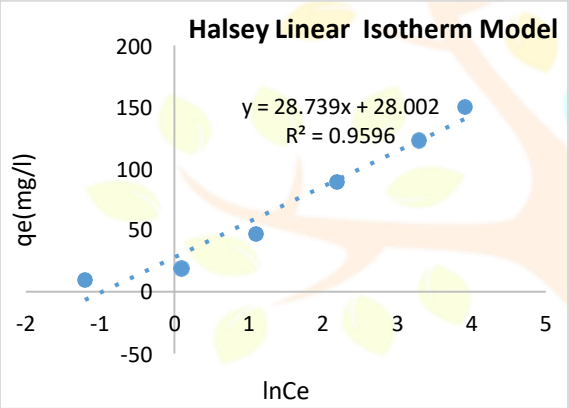

Figure 23: Halsey Linear isotherm on water hardness removal using NaSPR-MPS.

To create an equation that can be used to compare various adsorbents under various operational conditions and to plan and improve operating procedures, it is important to have equilibrium data for the adsorption process. An equilibrium process and a rate process may both be used to mathematically explain the mass transfer action known as adsorption. The amount of metal ions dissolved in the aqueous phase and the amount that is bound to the adsorbent are at an equilibrium (Bayramoglu.G, 2003).Temkin, Freundlich, Langmuir, Dubinin-Radushkevich, Hasley, and Redlich-Peterson (R-P) models were used to fit the experimental data to characterize the adsorption process' equilibrium. The plots for the adsorption of water hardness on the adsorbent and the findings displayed in the table above have been used to construct the constants of isotherm models as well as correlation coefficients (R2). With 5g of composite, a pH of 7 and a contact period of 150 minutes, adsorption equilibrium in the concentration range of 10 mg/l to 200 mg/l was examined. By raising the initial metal concentration in solution, the number of adsorbed ions steadily rises. After 150 mg/l of beginning concentration of water hardness, the rise starts to become consistent. This tendency is likely brought on by greater concentrations of the composite material saturating the adsorption site.

3.8.1 Langmuir isotherm

The Langmuir isotherm is perhaps the most used model, according to Dubinin (1997). The theory behind this modelimplies that the adsorbate covers the whole surface of the adsorbent in a monolayer.

The Linearized equation of Langmuir model is given as follows:

$$\frac{1}{qe} = \frac{1}{KL qmax Ce} + \frac{1}{qmax} \quad (4.4)$$

Where q_e is the amount of metal ions adsorbed onto adsorbent, C_e is the equilibrium concentration of water hardnessin solution, q_{max} and K_L are Langmuir constants related to adsorption capacity and adsorption energy respectively.

The q_{max} was calculated using the formula:

$$q_{max} = \frac{1}{\text{Intercept}} \quad (4.5)$$

KL was calculated using the formula:

$$KL = \frac{1}{\text{slope} \times q_{max}} \quad (4.6)$$

Rl was calculated using the formula

$$RL = \frac{1}{1 + C_i + KL} \quad (4.7)$$

3.8.2 Freundlich Isotherm

Affinity for the heterogeneous surface is assumed by the Freundlich isotherm to be non-uniform. heat distribution by adsorption. On heterogeneous locations, this model is utilized for multilayer adsorption (Freundlich.H, 1906). These are some ways that this model may be portrayed.

$$\log q_e = \log K_F + \frac{1}{n} \log Ce \quad (4.8)$$

where K_F represents the adsorption capacity (mg/g) n is a constant related to adsorption intensity. Linear plot of log qe versus log Ce shows the applicability of this isotherm for water hardness adsorption onto adsorbent.

3.8.3 Dubinin-Radushkevich (D-R) model.

This model is used, in accordance with Dubinin, to estimate the apparent free energy of adsorption. He also developed an equation to determine the adsorption process based on the potential theory and assuming a heterogeneous surface. the linearized from the provided D-R isotherm is

$$\ln C_{ads} = \ln X_m - \beta\varepsilon^2 \quad (4.9)$$

where C_{ads} is the amount of solute adsorbed per unit weight of solid

X_m (mg/g) is the adsorption capacity, β (mol/K)^2 is a constant related to energy and ε is the Polanyi potential. Polanyipotential can be computed by the following equation:

$$\varepsilon = RTln(\frac{1}{1+Ce}) \quad (4.10)$$

where R is a gas in KJ/mol and T is the temperature in Kelvin. If ln Cads is plotted against ε^2, β and X_m can be obtained from the slope and intercept respectively. The mean energy of adsorption (E) was calculated by the followingequation using the constant β

Isotherm constants and mean free energy of the Dubinin-Radushkevich. The adsorption capacity (X_m) of this model was calculated as

$$E=\frac{1}{\sqrt{-2\beta}} \quad (4.11)$$

The size of E is utilized to calculate the adsorption process' reaction mechanism. Value E that falls in the range of 1 to 8 kJ/mol denotes a physical adsorption. When E exceeds 8 kJ/mol, the adsorption process is chemical in nature.

3.8.4 Temkin isotherm

Pyzhev assessed the Temkin model, which presupposes a multilayer adsorption process and takes into account interactions between the adsorbent and the adsorbate but overlooks extremely high and very large concentration values. The Temkin isotherm is represented in its non-linearized form as follows:

$$qe = \frac{RT}{b} \ln(KmC_e) \quad (4.12)$$

where R is the universal gas constant in (J/mol K), T is the temperature in K, b is the Temkin constant related to sorption heat in J/mol and K_m is the Temkin isotherm constant in L/g .

According to the Temkin isotherm, adsorbent-adsorbate interactions cause the heat of adsorption of every molecule in the layer to drop linearly with coverage. Up to a certain maximum binding energy, the binding energies are distributed uniformly during adsorption. The Temkin equation is expressed in linear form as:

$$qe = \frac{RT}{bTe} InaTe \pm \frac{RT}{bTe} In\ Ce \quad (4.13)$$

where bTe is the Temkin constant related to heat of adsorption (J/mol); aTe the Temkin isotherm constant (L/mg),R the gas constant and T absolute temperature (K).The plot of the qe versus InCe gives straight line and bTe and aTe constants can be calculated from the intercept and slope(.

3.8.5 Redlinch-Peterson isotherms

This has three parameters. Adsorption isotherm does not display optimum monolayer adsorption behavior because it combines the traits of both the Langmuir and the Freundlich isotherm (Liu.Q, 2010). The Redlich-Peterson may be employed in both homogeneous and heterogeneous systems because it is a hybrid version. The model's mathematicalformulation is provided by:

$$q_e = \frac{KrCe}{1+aCe^{\wedge}\beta} \quad (4.14)$$

where K_r is the Redlich-Peterson isotherm constant in L/g α is the constant in L/mg and β is an exponent that ranges between 0 and 1.At low concentration($\beta \sim 1$) the model approaches the Langmuir and at high concentration ($\beta \sim 0$) itapproaches the Freundlich isotherm.

The linear for of the Redlich-Peterson isotherm is expressed as:

$$\ln(\frac{C_e}{q_e}) = \beta lnCe - lnKr \quad (4.15)$$

A plot of ln ($\frac{Ce}{qe}$) versus $\underline{\ln}C_e$ will provide β and K_r from the slope and intercept respectively.

3.8.6 Halsey Isotherm

At a considerable distance from the surface, the multilayer is evaluated using the Hasley isotherm. The model is appropriate for both multilayer adsorption and adsorption on heterogeneous surfaces. The R^2 value of it verifies the heterogeneity of sodium sulphonated polystyrene resin and powder from Moringa seeds as well as the potential for multilayer adsorption of water hardness on its surface. According to Ayawei, the experimental data for the adsorption of methyl orange on pinecone-derived activated carbon and Pb^{2+} ion on coconut shell carbon were well fitted to the Hasley isotherm. This was an excellent fit for the tested adsorbent's multilayer and heterogeneous distribution of activesites, at the very least. The presence of several groups, including

The adsorption can be given as follows:

$$q_e = \frac{1}{n_H} \ln K_H - \frac{1}{n_H} \ln C_{qe} \qquad (4.16)$$

where K_H and n are Hasley isotherm constant and they can be obtained from the slope and intercept of the plot $\ln q_e$ versus $\ln C_e$

The Freundlich isotherm has a strong correlation coefficient (R^2) value of 0.9712, which indicates that the composite model favors the Freundlich isotherm model. Multilayer adsorption is appropriate to the model. The Freundlinch isotherm model presupposes the involvement of many sites with various adsorption energies. It is well known that adsorption properties are best when n is between 2 and 10, challenging when n is between 1 and 2, and terrible when n is less than 1. In this work, Nasser-MSP demonstrated good adsorption characteristics with n > 3. Adsorption intensity or surface heterogeneity is measured by the slope 1/n, which has a range between 0 and 1. The surface becomes increasingly diverse as this value decreases toward zero. This study's 1/n value of 0.3543 indicates the surface's heterogeneity.

The values of R^2 for Freundlich obtained from this investigation were higher than those reported by Ridwan and Hamidin in 2011 for the removal of hardness using Moringa seed powder as an adsorbent, where the values for R2 for Langmuir and Freundlich were 0.5 and 0.7, respectively. When employing cash nut shell activated carbon as an adsorbent, Rolence (2016) achieved values for correlation regression that were higher. Redlich Peterson also endorsed the multilayer adsorption, which is applicable to both homogeneous and heterogeneous surfaces. The obtained value of was 0.4, which is closer to zero and supports the Freundlich isotherm hypothesis. The R^2 value for the Halsey isotherm was 0.9596, which was greater than the R^2 value for the Langmuir isotherm at 0.9461. The multilayer adsorption is also supported by the Halsey.Since E= 0.32 KJ/mol and the value is less than 8 KJ/ mol, Dubinin- Radushkevich demonstrated that the adsorption of water hardness on the composite of NaSPR-MSP favors physisorption. Redlich Peterson also backed the multilayer adsorption, which is applicable to both homogeneous and heterogeneous surfaces. The obtained value of was 0.4, which is closer to zero and favors the Freundlich isotherm model. R2 was greater for the Halsey isotherm (0.9596) than for the Langmuir isotherm (0.9461). The multilayer adsorption is supported by the Halsey as well. Since E= 0.32 KJ/mol and the value is less than 8 KJ/mol, Dubinin- Radushkevich demonstrated that the adsorption of water hardness on the composite of NaSPR-MSP favors physisorption.

Zero order	Slope	-0.1744
	Intercept	53.857
	R^2	0.8865
First order	Slope	-0.0053
	Intercept	4.0756
	R^2	0.9406
Second order	Slope	0.0002
	Intercept	0.0128
	R^2	0.9082
Pseudo Firstorder		
	Intercept	4.28817
	qe(mg/l)	72.83306197
	Slope	-0.02809
	K_1	- 0.000133762
	R^2	0.9014
Pseudo Second order	Intercept	0.01207
	qe(mg/l)	- 73182.33378
	Slope	-1.376E-05
	qe_2	5355653978
	R^2	0.78508

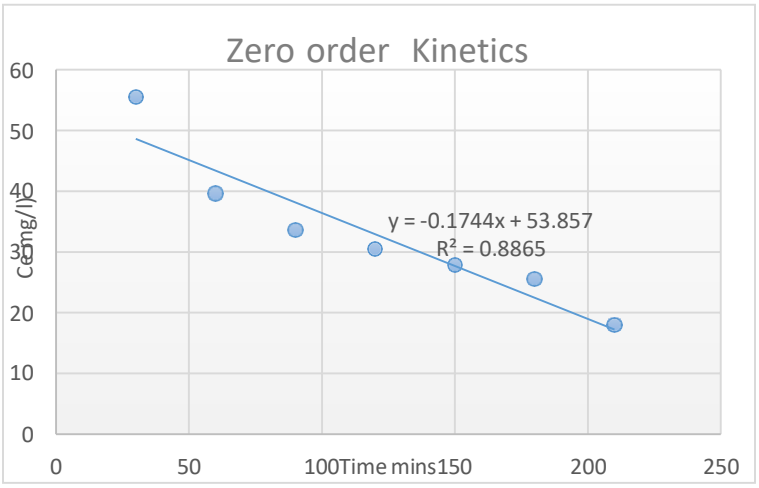

Figure 24: Zero order kinetics composite of NaSPR-MSP water hardness removal using composite of NaSPR-MSP

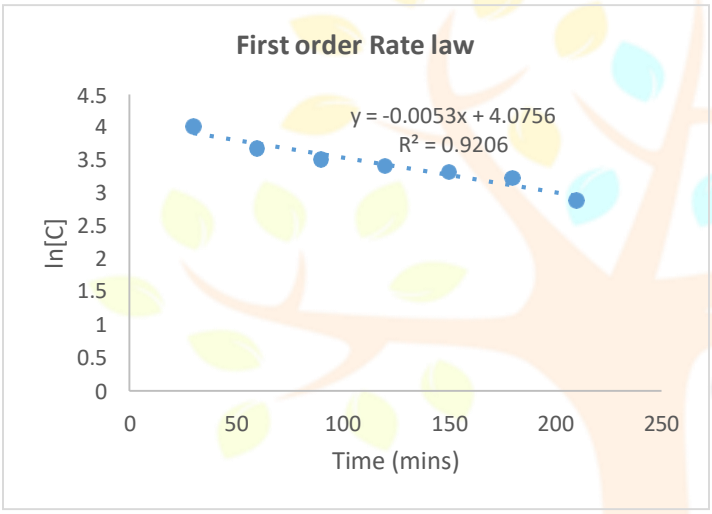

Figure 25: First order rate law of water hardness removal using composite of NaSPR-MSP

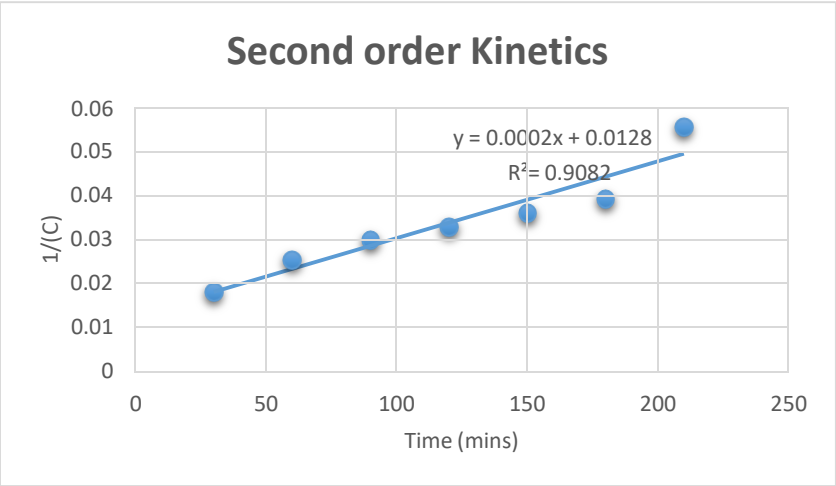

Figure 26: Second order kinetics on water hardness removal using composite of NaSPR-MSP

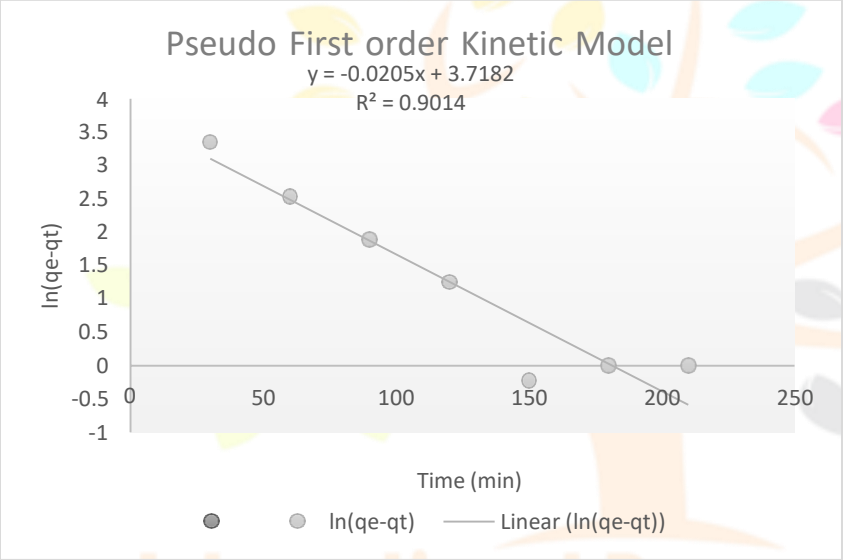

Figure 27: Pseudo first order kinetic on water hardness removal using composite of NaSPR-MSP

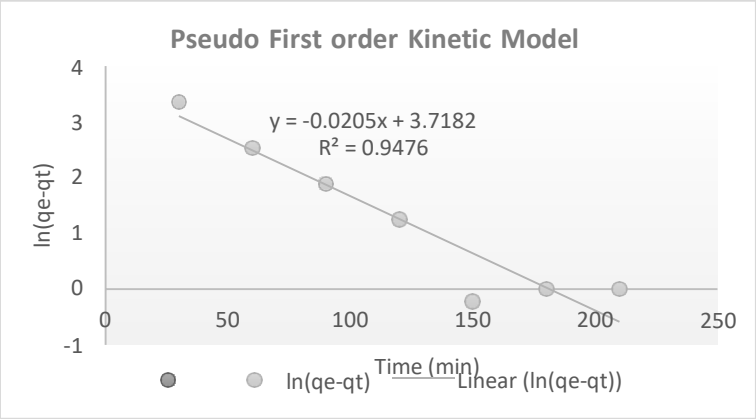

Figure 28: Pseudo First order kinetics on water hardness removal using composite of NaSPR-MSP

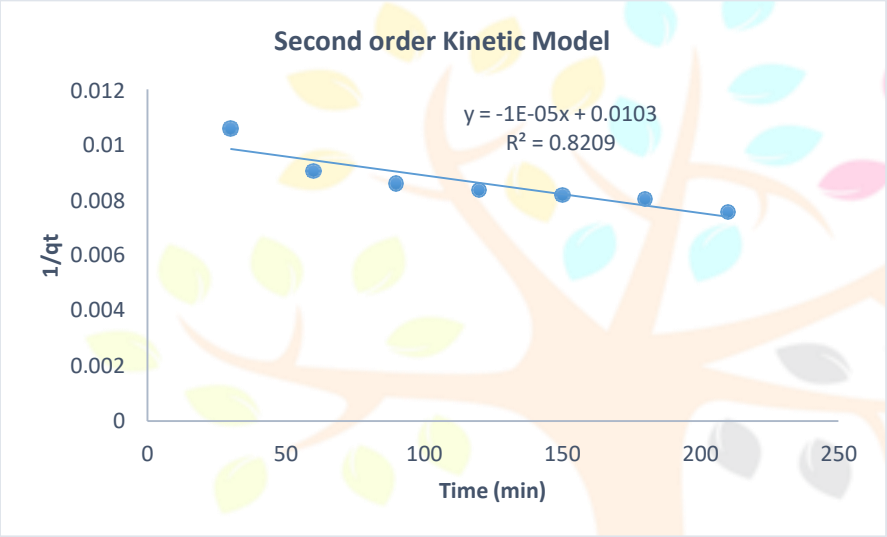

Figure 29: Pseudo second order kinetics on water hardness removal using composite of NaSPR-MSP

Due to the initial water hardness concentration's quick rise, the influence of contact duration on the adsorption of water hardness onto composite material was investigated between 10 and 210 minutes. Next, as the amount of time increases, the adsorption constants level out. The development of the adsorption capacity over time is depicted by the adsorption kinetic. Testing the experimental data to look for a potential rate-controlling step involved using zero order, first order, pseudo-first-order, and pseudo-second-order models. Kinetic factors for the process of adsorption of water hardness at various concentrations (YUsan.S, 2012).

3.8.7 Zero order kinetics on water hardness removal using composite of NaSPR-MSPThe equation of zero order:

$$[A]_t = -Kt + [A]_o \quad (4.17)$$

The equation has the general form for a straight line y=mx+ b so the plot of $[A]_t$ vs t is straight line with the slope (- k) and the intercept $[A]_o$

3.8.8 First order kinetics on water hardness removal using composite of NaSPR-MSP

The first order has the equation:

$$\ln[A]_t = -Kt + \ln[A]_o \quad (4.18)$$

Where $[A]_t$= concentration of [A] after some time, tk= reaction rate constant in units of min^{-1}

t=time in minutes

$[A]_o$= initial concentration of A.

This equation has the general form of a straight line y= mx + b. so the plot of $\ln[A]_t$ vs t is a straight line with slope (-k) and intercept $\ln[A]_0$

3.8.9 Second order kinetics on water hardness removal using composite of NaSPR-MSPThe equation of second order:

$$1/[A]_t = Kt + 1/[A]_o \quad (4.19)$$

Where $[A]_t$= concentration of [A] after some time, tk= reaction rate constant in units of min^{-1}

t=time in minutes

$[A]_o$= initial concentration of A.

This equation has the general form of a straight line y= mx + b. so the plot of $1/[A]_t$ vs t is a straight line with slope (-k) and intercept $1/[A]_0$

3.8.10 Pseudo-first order kinetic on water hardness removal using composite of NaSPR-MSPThe employed pseudo-first order

(Lagergren's) rate equation is given by;

$$\ln(q_e - q_t) = \ln qe - K_1 t \quad (4.20)$$

where qe is the amount of metal ion adsorbed onto adsorbent at equilibrium (mg/g),qt is the time of adsorption duration and k1 is the rate constant of the equation (min^{-1}) (Hammed.B.H, 2009).Slopes and intercepts of plots of ln(qe-qt) vs time were obtained for adsorbent to determine the first order rate constant k_1 at different water hardness concentrations.

3.9.5**.** Pseudo second order kinetics on water hardness removal using composite of NaSPR-MSP The pseudo-second-order model can be represented in the following form by:

$$\frac{t}{q_t} = \frac{1}{K_2 q_e} + \frac{1}{qe} \quad (4.21)$$

Where k_2 (g/mol min) is the second order rate constant. The linear plot of t/q_t as a function of t provided not only the rate constant k_2 but also an independent evaluation of qe. The pseudo-second-order rate constant k_2 was determined from the slopes and intercepts of plots of t/q vs t (YUsan.S, 2012).

where qe is the equilibrium adsorption capacity, where q_t is the amount of water hardness adsorbed and t is time, K_f is the pseudo first order rate constant and K_2 is the rate constant of pseudo second order kinetics according to Jethave et al (2017).

The first-order kinetic model's R^2=0.9406 correlation coefficients were found to be greater than those for zero order, second order, pseudo first order, and pseudo second order at various concentrations. For this reason, physical sorption or physisorption may be the rate-limiting phase (McKay.1940). Depending on the concentration of the two reactants, this may be the result of diffusion. In the scenario of two stages desorption, Atun and Sismanoglu reported. The sorption rate is regulated by either a film diffusion or an intra-particle diffusion mechanism, with the first step occurring more quickly than the second. This could be the case because the macroscopic and composite structure is probably more similar to a capillary system than a micro- or macro-porous honey comb. This monolayer approaches saturation a process of rearrangement may start with a further increase in the desorbate molecules which constitutes the second step. In order to calculate the adsorption rate for modeling and constructing the adsorption mechanism, Jayarathna et al. (2015) claim that numerous adsorption kinetics factors must be taken into account. The first order and second order models were used to analyze the kinetics of removing water hardness from sulphonated polystyreneresin and Moringa, respectively.

3.9.6 Intra-Diffusion Kinetic Model on water hardness removal using composite of NaSPR-MSPTable 4: Intra-diffusion Kinetic Model

Intercept	K_{diff}	R^2
87.077	2.9974	0.9671

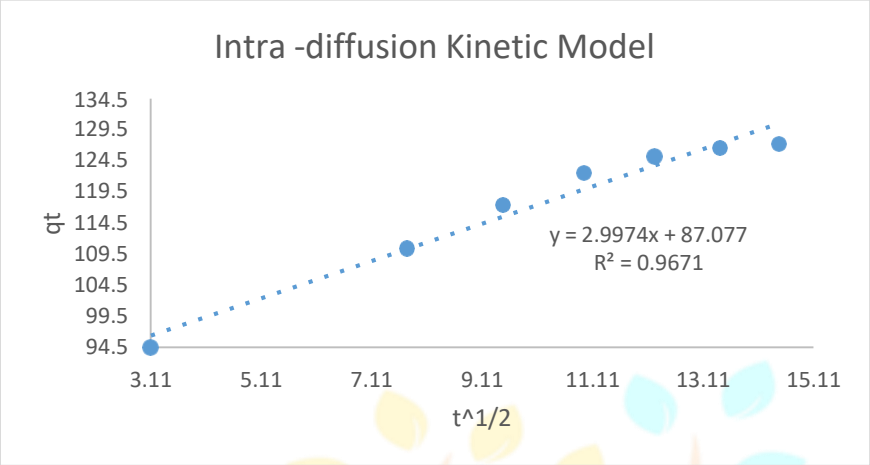

Figure 30: Intra-diffusion kinetic Linear Model on water hardness removal using composite of NaSPR-MSP.

Xu, Gao, Yue and Zhong (2010) reviewed that both zero order, first order, second order, pseudo first and second order cannot be used to identify the diffusion mechanism, but the intra particle diffusion was also proposed. The intra- particle was calculated using the equation:

$$Q_t = K_d\, t^{1/2} + C \qquad (4.22)$$

Where K_d is intra-particle rate constant (mg/l min-0.5) and it is a function of equilibrium concentration in solid phase, Q_t and the intra-particle diffusion C can be determined.

There are several mechanisms that regulate the adsorption kinetics, but diffusion, boundary layer diffusion, and intraparticle diffusion are the most restricting (Guibal E, 2003). The only rate-controlling step will be intra-particle diffusion when the line of intraparticle diffusion passes through the center (C=0). In this investigation, the plot of water hardness vs square root of time t1/2 did not pass through the origin, C= 87.077, indicating that intra particle diffusion was involved in the adsorption of water hardness. This demonstrated that other kinetic processes may also be active and contribute to the sorption mechanism, and intra-particle diffusion is not the only rate-limiting phase in the sorption process (Xu.X, 2010).

3.9.7 Thermodynamic studies on water hardness removal using composite of NaSPR-MSP Table 5: Thermodynamic parameters on water hardness removal using composite of NaSPR-MSP

Intercept	Slope	R(j/mo/l)	H=(j/mol/l	H=KJ/mol	S=j/k/mol
6.15293	968	8.31	8044.08	8.04408	51.13085

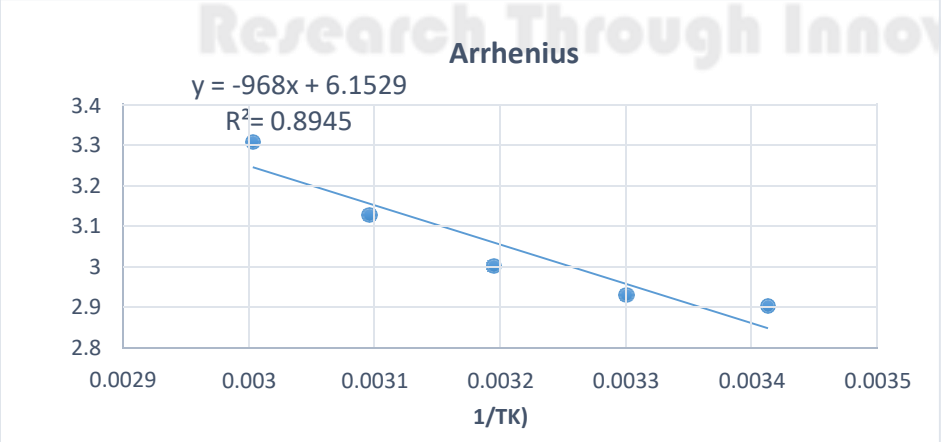

Figure 31: Thermodynamic plot for adsorption of water hardness on composite of Sodium sulphonated polystyrene resin and Moringa seeds Powder.

Thermodynamic parameters such as enthalpy change, entropy change and free energy change were estimated using the following equations:

$$In\ \frac{Kd}{R} = \frac{\Delta s^{\circ}}{RT} - \frac{\Delta H^{\circ}}{} \quad (4.23)$$

$$\Delta G^{\circ} = \Delta H^{\circ} - T\Delta S^{\circ} \quad (4.24)$$

Where Kd is the distribution coefficient, T is the temperature in Kelvin, and R is the gas constant (8.314J/mol K).The value of ΔH° and Δs° were dertemined from the slopes and the intercepts of the plots in InKd against 1/T for europium adsorption. Gibbs free energy (ΔG°) was calculated for each working temperature using equation distribution coefficient (Kd, mL/g) is also computed using the following equation:

$$\frac{Kd}{g}\left(\frac{mL}{Cem}\right) = \frac{Ci-Ce}{} \times \frac{v}{} \quad (4.25)$$

Where Ci and Ce are the initial and equilibrium concentrations of water hardness (mg/L) in solutions. m is the weight of the adsorbent (g).v is the volume of the aqueous phase (mL).The calculated values of the thermodynamic parametersfor the adsorption of water hardness.

The outcomes demonstrated the nature of the reaction mechanism as being endothermic. The study's findings indicated that the value of H was 8.041 KJ/mol. The positive values of the enthalpy change imply that the adsorption process is endothermic. The kind of adsorption can be considered as a physical process when H° is less than 40kJ/mol. The computed H° value for the adsorption of water hardness is 8.041 kJ/mol. This result indicates that physisorption is the adsorption reaction's mechanism. This outcome concurs with that of isotherm model simulations. S=51.13J/k/mol has positive entropy. The endothermic nature of the reaction was indicated by the positive value of for H. The increase in the degree of freedom (or disorder) of the adsorbed species is shown by the positive value of S. As temperature rises, the proportion of adsorption increases, indicating an endothermic process and the contrary. (Aytas, S.; Das, S.; 2009;2011).

Table 6: Gibbs free on water hardness removal using composite of NaSPR-MSP

ΔG (j/mol/l			
-482.7292611	-730.9232527	-998.3618481	-1299.967961

The adsorption process is thermodynamically viable, as evidenced by the negative values for the Gibbs free energy change, and the degree of spontaneity of the reaction rises with temperature. This suggests that at higher temperatures, the adsorption process is spontaneous and more favorable. The measured negative standard Gibbs energy changes show that the adsorption processes are strongly oriented toward the products.

The increase in adsorption with temperature may be ascribed to the desolvation of the sorbing species or an increase in the number of active surface sites on the adsorbents that are accessible for adsorption. The fact that S and H are positive and may be seen in spontaneous reactions at high temperatures indicates that the boundary layer's thickness reduces with temperature, which causes the adsorbate's mass transfer resistance to decrease in the boundary layer. This outcome is consistent with that of Mobasherpour, who used nanocrystalline tri-calcium phosphate to thermodynamically adsorb cadmium metal from aqueous solutions (Aytas.S, 2009; Das.S.K, 2011).

3.9 Application of composite in water hardness removal from Borehole water

3.10.1 Determination of water hardness

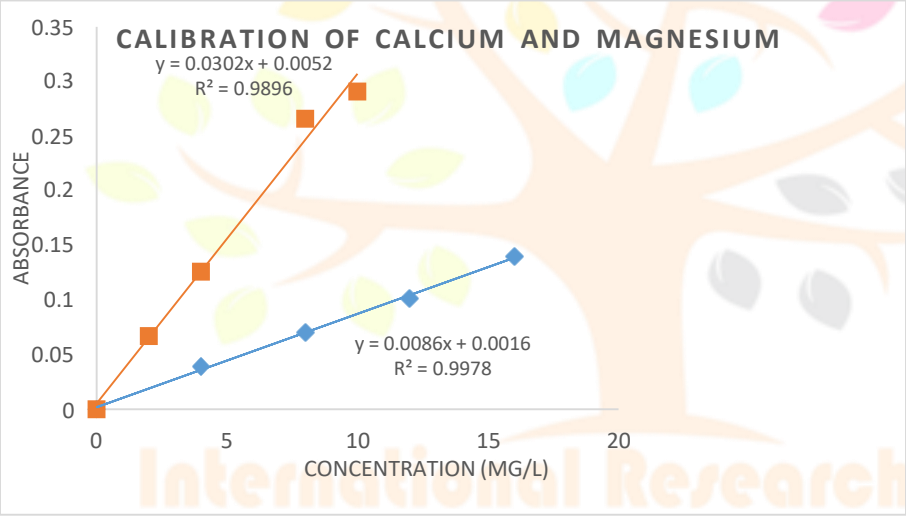

Figure 32: Calibration curves for determination of Calcium and Magnesium in water sample

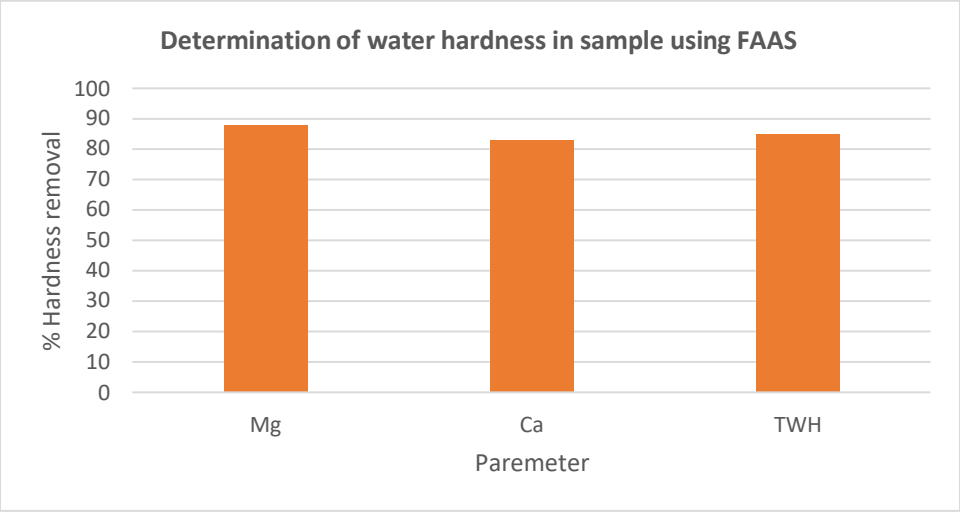

Figure 33: Determination of water hardness in water sample using FAAS

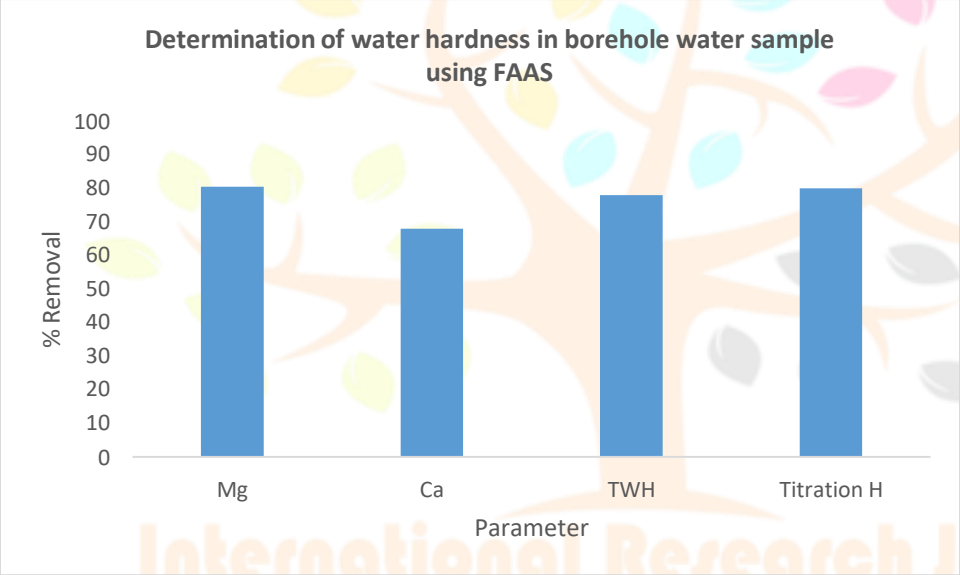

Figure 34: Determination of water hardness in borehole water sample using FAAS

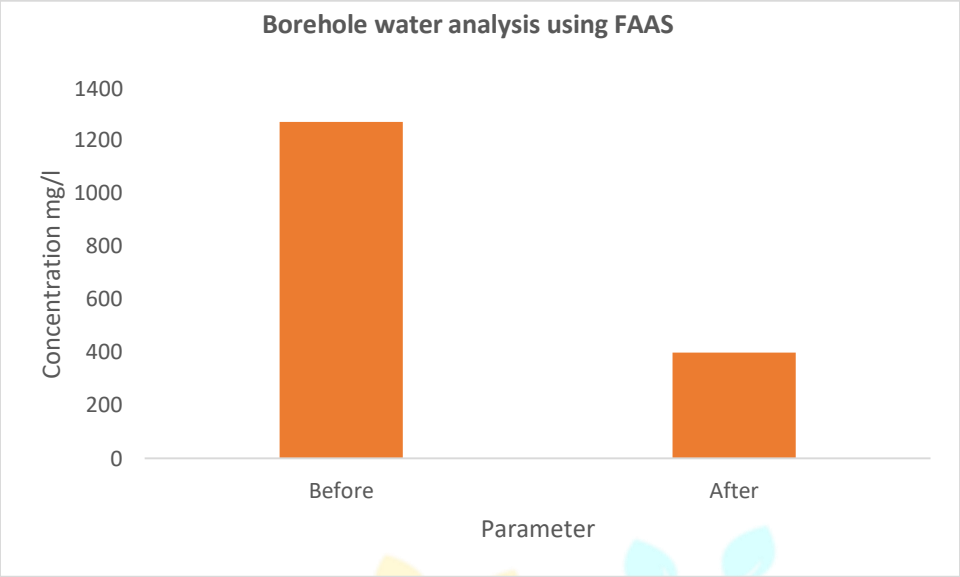

Figure 35: Borehole water sample analysis using FAAS

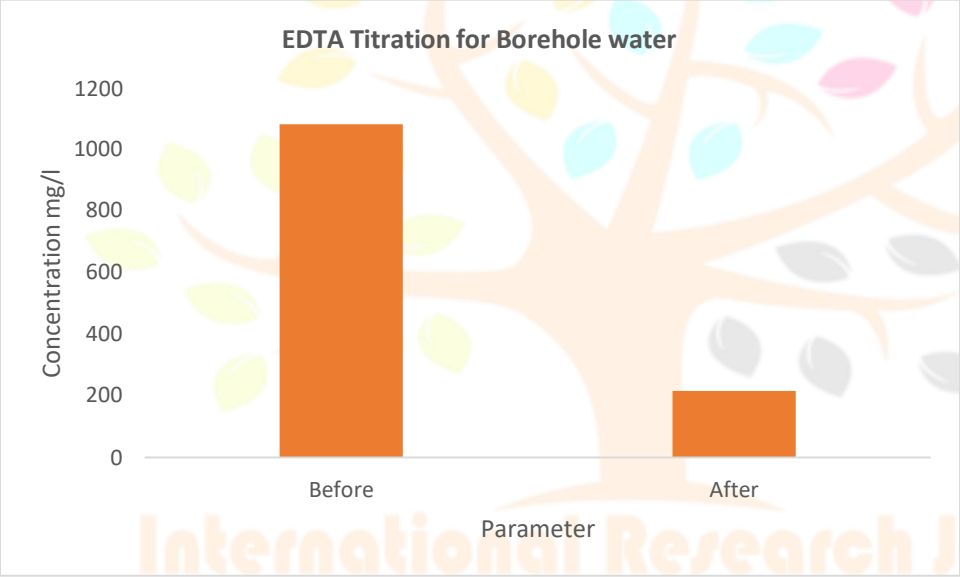

Figure 36: Borehole water sample analysis using EDTA Titration

Prior to adsorption, the total water hardness was determined to be 1080 mg/l and 1272 mg/l using the titration and FAAS methods, respectively. After adsorption, it was discovered that the total water hardness was 216 mg/l and 400 mg/l using the titration and FAAS methods, respectively. Using the FAAS and EDTA titration methods, it was discovered that the total amount of water hardness reduced from the bore water sample by the composite was 78% and 80%, respectively. In the prepared sample, 85% of the water hardness had been removed. According to the data above, magnesium had the highest percentage of elimination in both samples. The R^2 for calcium was found to be 0.9896, whereas the R^2 for magnesium was found to be 0.9978, indicating that the composite favors the adsorption of magnesium over calcium.

3.10.2 Determination of Chlorides in Borehole water

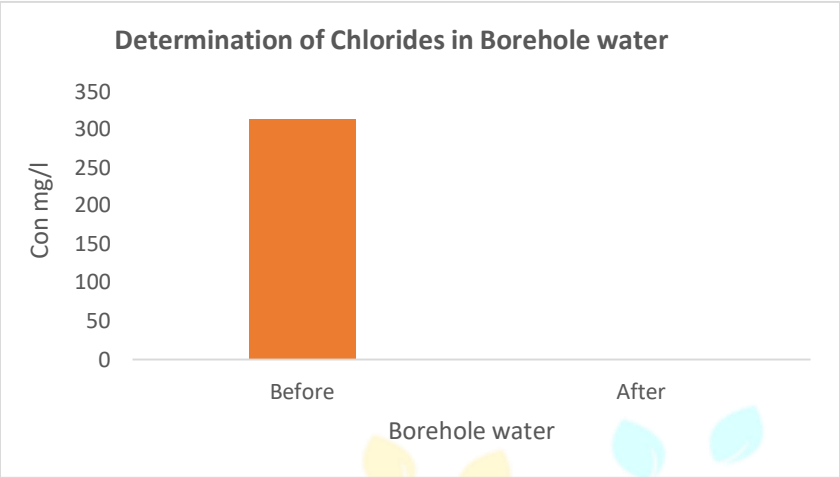

Figure 37: Determination of chlorides in borehole water sample using Mohr Titration

Before adsorption, the borehole water sample had 313.11 mg/l of chlorides, and it was discovered that the amount of chlorides was zero after adsorption. This suggests that every last trace of chlorides was eliminated from the sample.Ca, Mg, and Na chlorides are the sources of the water's chloride concentration. The fact that silver chlorides reacts with all chlorides precipitate before the interaction with chromate indicator forms the basis of the Argentomeric techniquefor the measurement of chlorides in water.

$$2AgNO_3 + Cl^- \longrightarrow AgCl + NO_3^- \quad (4.26)$$

When all the chlorides ions are precipitated as silver chlorides the excess drop of silver react with chromate ions to form a brick- red precipitation.

$$2AgNO_3 + CrO_3^{2-} \longrightarrow \underset{\text{Brick red colour}}{Ag_2CrO_4} + NO_3^- \quad (4.27)$$

The appearance of brick-red colour of silver chromate precipitate is the endpoint of titration. The reaction between silver nitrate

3.10 Conclusion and Recommendation

3.10.1 Conclusion

Using a composite of NaSPR-MSP, it was possible to study the softening of hard water by eliminating Ca2+ and Mg 2+. Utilizing FTIR, TGA, and XRD, the composite's structure was verified. The elimination of cations increased with increasing adsorbent mass, contact time, or beginning ions concentration. With an R^2 of 0.9712, the adsorption favors the Freundlinch isotherm..First order kinetic model was discovered to have R^2= 0.9406 as its value. As the graph did not pass through the origin, the diffusion mechanism was caused by intra-particle diffusion and other kinetic processes. Because the value of H=8.041KJ/mol, thermodynamic analyses indicated that the reaction was endothermic. Since H was less than 40 kJ/mol, this evidence further supported the notion that physisorption was at work. A rising level of freedom for adsorbed species is shown by the positive s. This shows that temperature-dependent adsorption increases. The process of adsorption is thermodynamically possible, as evidenced by the negative value for the Gibbs free energy, and the degree of spontaneous rise with temperature. Before adsorption, 1080 mg/l and 1272 mg/l of total water hardness were observed in borehole water. Using the titration and FAAS methods, it was discovered that the concentration was 400 mg/l and 216 mg/l, respectively, after adsorption. This helps to remove water hardness by 78%

and 80%, respectively. Total chlorides were determined to be 313.11 mg/l prior to adsorption and 0 mg/l following adsorption, showing that all chlorides were eliminated from the water.

3.11 Recommendation

The author suggests that waste polystyrene be collected and recycled for use in removing water hardness by creating a composite out of NaSPR and MSP.To establish the composite's potential for removing microorganisms, more research on it is necessary. It is also important to investigate the composite's capacity for adsorption of additional anion species, such as sulfate and nitrates. It is important to investigate both the regeneration mechanism and the composite's lifespan.

References

[1] Andrad AL, N. M., 2009. Application and societ benefits of plastics.. *Phsilosphical Translation of Royal Society Of London B Biological Sciences*, 364(1526), pp. 1977-84.

[2] Anwa, f. a. R., 2007. Physico-chemical characteristics of Moringa Oleifera seeds and seeds oil from a wild provenance of Pakistan. *J.Bot*, pp. 1443-1453.

[3] Apell, J. B. T., 2010. Combined ion exchanged treatment fro removal of dissolved 0rganic matter and hardness. *Water Res*, Volume 44, pp. 2419-2430.

[4] Ayawei.N, E. a. W., 2017. "Modelling and interpretation of adsorption iostherms". *Journal of Chemistry*, Volume 11. page 345

[5] Aytas.S, Y. a. D., 2009. "Adsorption characteristic of U(V1) ion onto thermally activated bentonite". *J.Hazard Mater*, 172(2-3), pp. 667-674.

[6] Bandyopadhyay Abhijit, C. B. G., 2007. "Studies on photocatalytic degradation. . *Materials Science and Technology 23 (3)*, 23(3).

[7] Bayramoglu.G, 2003. "Biosorption of heavy metal ions on immobilized white -rot fungus trametes versicolor".. *J.Hazard. Matter* ., 101(3), pp. 285-300.

[8] Bekri-Abbes, B. B., 2007. *The removal of hardness of water using sulfonated waste plastic*, s.l.: Science Direct.

[9] Bekri-Abbes, L. S. a. B., 2006. "Converting waste polystrene into adsorbent:potential use in the removal of leasd and cadium ions from aqueous solution". *Journal of Environmental Polymer Degradation*, 14(Dol 10.1007/s10924- 006-0018-3), pp. 249-256.

[10] Berger.M, H. a. S., 1984. "Toxicological assessment of seeds from Moringa oleifera stenopetala, two highly efficient primary coagulants for domestic water treatment of tropical raw waters". *East Africa Medical Journal* , 61(9),p. 712.

[12] Bozkurt.A, 2005. Turk. *J.Chem*, Volume 29, pp. 117-123.

[13] Camel.V, 2001. 'Recent extraction techniques for solid matruces-supercritical fluid extraction, pressured fluid extraction and microwave-assisted extraction: their potential and pitfalls". *Analyst*, 126(7), pp. 1182-1193.

[14] Campbell.B.M, 1987. The Use of Wild Plants in Zimbabwe. *Economic Botany* , 41(3), pp. 375-385.

[15] Chumark.P, e. a., 2008. 'The in vitro and ex vivo antioxidant properties, hypolipidaemic and antiatherosclerotic acivities of water extraction of Moringa oleifera Lam leaves". *Hournal of ethnopharmacology*, 116(3), pp. 439-446.

[16] Das.S.K, S. a., 2011. "Biosorption of Cr(V1) ions from aqueous solution:Kinetics, equilbrium , thermodynamics and desorption studies". *Colloids surface B Biointerface*, 84(1), pp. 221-232.

[17] Dean.J.A, 1995. *Dean's Analytical Chemistry Handbook.* second ed. New York: (McGraw-Hill Handbook).

[18] Dimirkou, A., 2008. Use of clinoptilolite and an Fe-overexchange clinoptilolite in Zn2+ and Mn 2+ removal from drinking water. *Desalination*, 224(1-3), pp. 280-292.

[19] Dubinin.L.V, Z. a. R., 1947. "Sorption and strcucture of active carbon. Adsorption of organic vapors". *Zhurnal Fiz. Khimii* , Volume 21, pp. 1351-1362.

[20] Durlak S, B. S. B., 1998. Characterization of polycyclic aromatic hydrocarbon particulate and gaseous emmissions from polystyrene combustion. *Environmental Science and Technology* , Volume 32, pp. 2301-7.

[21] Elimelech.M., M. a., 2007. "Water and sanitation in developing countrie: Including health in the equation. *ACS Publications*, pp. 17-24.

[22] Faghihia.H, M. &. K., 1999. The use of clinoptilolite and its sodium form for removal of radioactive caesium and strotium from nuclear wastewater adn Pb++, Ni++, Cd++, Ba++ from municipal wastewater. *Appl.Radiat*, Volume 4,pp. 655-661.

[23] Fahey.J.W., 2005. "Moringa Oleifera: a review of the medical evidence for its nutritional , therapeutic, and prophylatic properties. Part 1. *Trees for life Journal* , 1(5), pp. 1-15.

[24] Fahey.J.W, Z. a. T., 2001. "The Chemical diversity and distribution of glucosinolates and isothiocyannates among Plants". *Phytochemistry* , 56(1), pp. 5-51.

[25] Falchuk.K.H, 1974. A multichannel atomic absorption instrument: Simultaneous analysis of zinc, copper and cadmium in biological materials.. *Anal.Biochem*, Volume 62, pp. 255-267.

[26] Farooq.F, R. K. a. F., 2012. "Mediccinal properties of Moringa Oleifera: An overview of promising healer". *Medicinal Plants Research* , 6(27), pp. 4368-4374.

[28] Fassel.V.A, 1969. Measuring trace elements. *science*, Volume 164, pp. 819-820.

[29] Ferrao.J, F. a., 1970. "Fatty acids of the oil of Moringueiro (Moringa oleifera (M.pterygosperma). *Agron.Angolana*, Volume 30, pp. 3-16.

[30] Foidl.N, M. a. B., 2001. *'Potentiel de Moringa Oleifera en agriculture et dans I'industrie,Potentiel de developpement des produits de Moringa,* Dar es-Sallam Tanzanie: s.n.

[31] Forsyth.B, C. a. M., 1995. "Explosives and water quality"',In Proceedings of Sudbury 95 Mining and the Environment. *Mine Environment Neutral Drainage,* pp. 795-803.

[32] Foster, S. H. &. G., 2010. Urban Groundwater Use Policy-Balancing the Benefits and Risks in Developing Nations.GW-MATE strategic overview serries.

[33] Freundlich.H, 1906. "Adsorption in solution ". *Zeitschrift fur Phys.Chemie*, Volume 57, pp. 384-410.

[34] Fuglie.L.J, 1999. *The Miracle tree:Moringa Oleifera , natural nutrition for the tropics,* s.l.: Available on :agris.fao.org.Accesse 13/07/2022.

[35] Fu, L., 2009. Removal of low concentration of hardness ions from aqueous solution using electrodeionization process. *Sep.Purif.Technol*, 68(3), pp. 390-396.

[36] Furton.K, A. a. W., 2000. "Application of solid-phase microextraction to the recovery of explosives and ignitable liquid residues from forensic specimens'. *Journal of Chromatography*, 885(1), pp. 419-432.

[37] Ghasi.S, N. a. O., 2000. "Hypocholesterolemic effects of crude extract of leaf of Moringa oleifera Lam in high- fat diet fed Wistar rats. *Journal of ethnopharmacology*, 69(1), pp. 21-25.

[38] Ghorbani.F, Y. e., 2008. Application of response surface methodology for optimization of cadmium biosorption in an aqueous solution by Saccharomyces cerevisiae. *Chemical Engineering Joiurnal* , Volume 145, pp. 267-275.

[39] Gleick, P., 2003. The human right. *Water Nepal*, 9-10(1-2), pp. 115-149.

[40] Gleick, W., 2003. The human rights to water. *Water Nepal*, 9-10(1-2), pp. 115-149.

[41] Gleiner. H, E. W., 2003. Optimization of analytical performance of a graphite furnance atomic absorption spectrometer with Zeeman-effect background correction using variable magnetic field strenght. *Spectrocheical Acta Part B:Atomic spectroscopy*, Volume 58, pp. 1663-1678.

[42] Guibal E, M. a. T., 2003. Comparison of the sorption of anionic dyes on actvated carbon from dilute solution. *Sep Sci Technol*, Volume 38, pp. 3049-3073.

[43] Guida.M, e. a., 2014. "Toxicity evaluation of alumin-coagulation municipal wastewater to sea urchin embroygenesis and fertilization'. *Desalination and Water Treatment* ., 52(16-18), pp. 3004-3011.

[44] Hammed.B.H, S. a. A., 2009. "Adsorption isotherm and Kinetic modeling of 2.4-D pestricide on activated carbon derived from date stones". *J.Hazard Matter.*, 163(1), pp. 121-126.

[45] Haris.D.C, 2010. *QUalitative chemical analysis.* 8th ed. New York: Clancy Marshal.

[46] Harris.D.C, n.d. *Quantitative Chemical Analysis.* s.l.:s.n.

[47] Hocking.M.B, 1991. Paper versus polystyrene. *A Complex choice* , 251(4993), pp. 504-5.

[48] Idibie.C.A., 2009. *Doctoral Thesis: Suphonation of synthetic Rubber As An Alternative Membrane For Proton Excchange Membrane Fuel Cell.*, Johannesburg, South A frica: University of Witwater, .

[49] Jahn.S.A.A, 1988. 'Chemotaxonomy of flocculating plant materials and their application for rural water purification in developing countries". *Symbolae Botanicea Upasalienses (Sweden),* Volume 28, pp. 186-188.

[50] Jancar.J, K. F. a., 1996. 'Preliminary study of Sulphonation of Polystrene by Homogenous and Heterogenous Reaction. *Chem Papers,* 50(4), pp. 224-227.

[51] Kazemian.H, M. M., 2003. Evaluating the performance of an Iranian natural clinoptilolite and its synthetic zeolite P for removal of Cerium and Thorium from nuvlear waste waters.. *J.Radional.Nucl.Chem,* Volume 258, pp. 551-556.

[52] Kirkman, A. C., 1991. *'Recycling Plastics Today',* s.l.: Chemtech.

[53] Koirtyohann.S.R, P. E., 19965. Background corrections in long path atomic absorption spectrometry. *Analytical Chemistry,* 37(4), pp. 601-603.

[54] Kucera.F, J. a., 1996. "Preliminary Study of Sulfonated Of Polystrene by Homogenous and Heterogenous Reaction'. *Chem papers,* 50(4), pp. 224-227.

[55] Lerner, D. &. H., 2009. The relationship between use and groundwater resources and quality. *Land use Policy,* Volume 26.

[56] Lewen.N, 2011. The use of atomic spectroscopy in the pharmaceutical industry for the detection of trace elements in pharmaceuticals. *J.pharm.Biomed. Anal ,* 55(4), pp. 651-653.

[57] Li.L, Z. a. W., 2003. J.Membr. *Sci,* Volume 226, pp. 159-167.

[58] Li, C. L. J. L. Y., 2005. Integrating a membrane and a fluidized pellet reactor for removing hardness effects of NOM and posphate. *Desalination,* Volume 175, pp. 279-288.

[59] Liliana.L, 2014. FTIR analysis of ion exchange resins with application in permanent hard water softening.. *Environmnetal Engineering and Management Journal,* 13(9), pp. 2145-2152.

[60] Lilian, L. R.-E. T.-F. M. G., 2014. FTIR analysis of ion exchange resins wiyth application in permanent hard water softening.. *Environmental Engineeriong and Management Journal,* 13(9)(DOl:10.30638/EEMJ.2014.237).

[61] Liu.Q, Z. T. W. P. J. L. N., 2010. Adsoption isotherm, Kinetics and Mechanism Studies of some substituted Phenols on Activated Carbon Fibres. *Chem .Eng.J,* 157((2-3)), pp. 348-356.

[62] Locette.C.C.C, 2000. 'Energy and micronutrients composition of dietary and medicinal wild plants during drought. Study of rural Fulani, Northen Nigeria'. *International Journal of food science and nutrition,* 51(3), pp. 195- 208.

[63] Maicaneanu.A, V. B. a. G., 2014. "Physical-chemical and elctrochemical characterization of Fe-exchange natural zeolite applied for obtaining of hydrogen perioxide amperometric sensors". *Geochemistry,* 74(4), pp. 653-660.

[64] Margat, J. &. V. d. G. J., 2013. *Ground water aroumd the World: A Geographic Synopsis.* Balkema: CRC Press.

[65] Margat, J. &. V. d. G. J., n.d. *Ground water around the World:Geographic Synopsis.* s.l.:s.n.

[66] Matshediso.P.G, 2015. *'Development of pressurised hot water extraction (PHWE) for essesntial components from Moringa Oleifera and Ovalifolia leaves'(Master Dissertation),* s.l.: s.n.

[67] Mau.J, e. a., 2007. *"Polystyrene and styrene Copolymer"in Ullmann's Encyclopedia of Industrial Chemistry.* Weinheim: Wiley -VCH, .

[68] McKay., H. a., 1940. "Pseudo- second order model for sorption processes". *Process Biochem,* 34(5), pp. 451- 465.

[69] MIchael.R, W. a. M., 1988. 'Glow Discharge Sputter Atomization for Atomic Absorption Analysis of Nonconducting Powder Samples'. *Applied Spectroscopy,* 42(6), pp. 941-944.

[70] Mukanga, C. M. B. C. T., 2016. An analysis of ground water quality in a water stressed urban center:A case of Gweru City Zimbabwe. *Water Practice & Technology,* June.

[71] Mulijani.S, D. a. W., 2014. INT.J.Mater. *Mech.Manu,* Volume 2, pp. 36-40.

[72] Ndabigengesere.A, N. a. T. (., 1995. 'Active agents and mechanism of coagulation of turbid water using Moringa olefeira'. *Water Research,* 29(2), pp. 703-710.

[73] Ndabigengesere.A, N. a. T., 1998. "Use of Moringa Oleifera seeds as a primary coagulant in wastewater treatment'. *Environmental Technology,* 19(8), pp. 789-800.

[74] Nhamo.C, e. a., 2016. *Potential uses amd value added products derived from waste polystyrene in developing countries with emphasis on sub-Saharan Africa*, s.l.: s.n.

[75] Palada.M.C, 19996. "Moringa (Moringa oleifera Lam): A versatile tree crop with horticulture potential in the sobtropical United States.". *HortScience* , 31(5), pp. 794-797.

[76] Paliwal.R, S. a., 2013. 'Isolation and characterization of saponins from Moringa oleifera (moringaceae) pods. *Int J Pharm Scie*, 5(1), pp. 179-183.

[77] Palmer.B & Pitman.N, 1972. *Trees of Southern Africa.* Vols 1 and 2 ed. Cape Town: AA Balkema.

[78] Pandey.A, T., 2014. Concept of Standardization, extraction and pre phytochemical screen strategeies for herbal drug. *Journal of Pharmacognosy and Phytochemistry* , 2(5), pp. 115-119.

[79] Pant, B., 2011. Ground water quality in the Kathmandu valley of Nepal. *Environmental Monitoring and Assessment* , Volume 178, pp. 477-485.

[80] Park, J. Y. k. M., 2009. Reomoval of hardness ions from tap water using electrodeionization process. *Sep .Purif. Technol*, 68(3), pp. 390-396.

[81] Plonke, H. &. U., 1985. Effect of agriculture land use on ground water quality in a small Pennsylvania watershed. *Groundwater*, 23(1), pp. 68-80.

[82] P, S. a. J., 1982. 'Clinical assessment of sigru (Moringa oleifera Lam.) on mutrakrichra (lower urinary tract infection}.. *Nature*, 10(1), pp. 231-235.

[83] Pyzhev, T. a., 1999. 'Recent modifications to Langmuir isotherms". *Acta Physiochim*, Volume 12, pp. 451-465.

[84] Quan, J., June 13 2006. *"Letter to Public Works Commitee*, California: Oakland .

[85] Radnia.H, G. Y. e. a., 2012. Adsorption of Fe(II) ions from aqueous phase by chitosan adsorbent: Equilbrium,Kinetic and thermodynamic studies.. *Desalination and water Treatment* , Volume 50, pp. 348-359.

[86] Ramachandandran.C, P. a. G., 1980. "Drumstick (Moringa oleifera): a Multipurpose Indian vegetable". *Econnomic Botany*, 34(3), pp. 276-283.

[87] Ramachandran.C, P. a. G. P., 1980. 'Drumstick (Moringa oleifera):a multipurpose Indian vegetable'. *Economic Botany*, 34(3), pp. 276-283.

[88] Rao, e., 2004. Conjuctive use of surface and groundwater for coastal and deltaic systems. *Journal of water Resources Planning and Management*, 130(3), pp. 255-267.

[89] Research, C. o. S. a. i., 1962. The Wealth of India. *A dictionary of Indian raw materials and industrial products*, Volume Vi, pp. 425-429.

[90] Research, C. o. S. a. I., 1962. The Wealth of India. *A dictionary of Indian raw materials and Industrial products*, Volume Vi, pp. 425-429.

[92] Rockerb.R.A, E. a., 1972. Semiautomated colorimetric determinationof glycerides. *Clin.Biochem*, Volume 50, pp. 503-508.

[93] Schot, P. &. P., 2012. Spatial and temporary variations in shallow wetland groundwater quality. *Journal of Hydrology*, Volume 422-423, pp. 43-52.

[94] Schot, P. P. S., 2012. Spatial and temporal and temporal variation in Shallow wetland groundwater quality. *Hydrology*, Volume 422-425, pp. 43-52.

[95] Seifi.L, T. K. B. A. N., 2011. Adsorption of BTEX on surfactant modified granulated natural zeolite nanoparticles:parameters optimizing by applying Taguchi experimental design method. *Clean-Soil, Air, water*,Volume 39, pp. 939-948.

[96] Seo.S.J, e., 2010. Investigation on removal of hardness ions by capacitive deionization (CDI) for water softening application. *Water Res*, Volume 44, pp. 2267-2275.

[97] Shan.T.C, M., 2017. 'The use of Moringa oleifera seed as a natural coagulant for waste water treatment and heavy metals removal. *Applied Water Science*, 7(3), pp. 1369-1376.

[98] Shelkholeslami, R., 2011. Composite Scale formation and assessment by theoretical scaling Potential index (SPI) proposed previously for a single salt. *Desalination*, 278(1-3), pp. 259-267.

[100] Shrestha, I. a. S., 20011. Statistical models and water quality characterization of source waters in Nepal. *Journal of Science and*

Technology, Volume 12, pp. 260-267.

[101] Shukla.S, a. e., 1988. 'Antifertility profile of the aqueous extract of Moringa oleifera roots'.. *Journal of Ethnopharmacology*, 22(1), pp. 51-62.

[102] Sismanoglu, A. a., 1996. Adsorption of 4,4'- isopropylidene diphenol and diphenylolpropane 4,4' dioxyaceicacid from aqeous solution on Kaolinite. *Environmental Science and Health Part A* .

[103] Sivakumar.V, A. S. a. G., 2014. Removal of Congo Red Dye using an Adsorbent Prepared from Martynia annuaL Seeds. *American Chemical Science Journal* , 4(4), pp. 424-442.

[104] Smith.R.B, H. G., 1983. A new background correction method for atomic absorption spectroscopy. *Applied Spectroscopy*, 37(4), pp. 419-424.

[105] Soren, S. M. &. C. P., 2011. Safe access to safe water in low income countries:water fetching in current times. *Social Science and Medicine*, Volume 72, pp. 1522-1526.

[106] Soren, S. M. &. C. P., n.d. Safe access to water.

[107] Suzuki, K. T. ,. T. O. T. a. W. M., 2002. Reomaval of phosphate , magnesium and calcium from swine wastewater through crystallization enhanced by aeration. *Water Research* , Volume 36, pp. 2991-2998.

[108] Tamrakar, C. a. S., 2013. Physico-Chemical assessment of deep ground water quality of various sites of Kathmands Metropolitan City, Nepal.. *Research Journal of Chemical Sciences*, Volume 3, pp. 78-82.

[109] Teo.C.C., e. a., 2010. 'Pressurized hot extraction (PHWE). *Journal of Chromatography A.Elsevier B.V*, 1217(16), pp. 2484-2494.

[110] Torabian.A, K. S. A. G. S., 2010. Removal of Petroleum Aromtic Hydrocarbon by surfactant-Modified Natural Zeolite. *Clean*, Volume 38, pp. 77-83.

[111] Trezek.G, e. a., 1993. *'Polystrene recycling process'*, s.l.: s.n.

[112] UNICEF, W. a., 2012. *Progress on drinking water and sanitation* , s.l.: s.n.

[113] UNICEF, W. a., 2012. *Progress on drinking water and sanitation* , s.l.: s.n.

[114] Vallee.B.L, F. a., 1963. Thmbert physical basis of analytical atomic absorption spectrometry.The pertinence of Beer-Lambert Law. *Anal.Chem*, Volume 35, pp. 942-946.

[115] Van Der Hoven, S. S. D. a. M. G., 2004. Natural spatial and temporal variation in groundwater chemistry in fractured, sedimentary rocks: Scale and implicatioons for solute trasnsport. *Applied Geochemistry*, 20(5), pp. 861- 873.

[116] Verdcourt.B, 1985. *A synopsis of Moringaceae*, s.l.: Kew Bulletin.

[117] Vink.H, 1981. Sulphonated Polystyrene. *Macromol Chem* , Volume 182, p. 279.

[118] Walsh.A, 1974. Atomic Absorption Spectroscopy-stagnant or pregnant. *Analytical Chemistry*, 46(8), pp. 698A-708A.

[119] Wang.J.Peng.Z., H., 2004. 'Growth of magnetite nanorods along its easy-magnetization axis. *Journal of crystal growth*, 263(1), pp. 616-619.

[120] Wang.Q, L. a. L., 2016. Desalination. *Desalination*, Volume 390, pp. 33-46.

[121] Wang.X, z., 2005. A general strategy for nanocrystal synthesis. *Nature*, 437(7055), pp. 121-124.

[122] Xu.X, G. Y. Q.-Y. a. Z.-Q., 2010. Preparation and utilization of wheat straw bearing amine groups for the sorption of acid and reactive dyes from aqueous solutions. *Journal of Hazardous Materials* , 182((1-3)), pp. 1-9.

[123] YUsan.S, G. E. a. A., 2012. "Adsorptive removal of thorium (1V) using calcined and flux calcined diatomite From Turkey:Evaluation of equilibrium, Kinetic and thermodynamic data". *Appl.Clay Sci*, Volume 67-68, pp. 106- 116.